THE EFFECT OF TEMPERATURE ON THE FORMATION AND ANNIHILATION OF POSITRONIUM IN POLYMERS

By

GERALD DEAN LOPER, JR.

Bachelor of Arts
University of Wichita
Wichita, Kansas
1959

Master of Science
Oklahoma State University
Stillwater, Oklahoma
1962

Submitted to the Faculty of the Graduate School of
the Oklahoma State University
in partial fulfillment of the requirements
for the degree of
DOCTOR OF PHILOSOPHY
August, 1964

THE EFFECT OF TEMPERATURE ON THE FORMATION AND ANNIHILATION OF POSITRONIUM IN POLYMERS

Thesis Approved:

B. Clark Groseclose
Thesis Adviser

H. E. Harrington

K. D. Berlin

Leon W. Schroeder

E. E. Kolumbus

J. H. Boggs
Dean of the Graduate School

PREFACE

The long, 10^{-9} second lifetime component of positrons in molecular materials is due to the formation of the bound electron - positron system, positronium, in the triplet state followed by the annihilation of the positron with a lattice electron of opposite spin. The formation of positronium depends on the amount of free or empty volume available to it, which may be expected to change with temperature.

The above - mentioned τ_2 component was measured in three polymers over the temperature range -196°C to +150°C, which includes at least one phase transition for each polymer. The data were compared to changes in physical properties of the polymers in the same temperature range. Although the usefulness of such measurements as a solid state tool is uncertain, it is hoped that they may lead to a clearer picture of molecular dimensions and structures.

The author acknowledges his gratitude to his major adviser, Dr. B.C. Groseclose for his assistance and guidance and to Dr. K.D. Berlin and Dr. E.E. Kohnke for valuable discussions and suggestions. Mr. Lewis P. Keller, Mr. Jack E. Houston, and Mr. Howard F. Kunkle occasionally watched over the equipment, and Mr. Benard A. Sodek and Mr. Tom L. Thomason gave advice concerning the use of the 650 and 1620 computers, for which the author is also grateful. Mr. Heinz Hall, Mr. Frank Hargrove, and Mr. Richard Gruhlkey of the Physics Shop were most helpful in preparing the samples and sample holders. The author

also appreciates the unstinting help and understanding of his wife, Joyce Loper, who typed the thesis.

This work was supported in part by an Army contract.

TABLE OF CONTENTS

LIST OF TABLES

LIST OF FIGURES

CHAPTER I

THEORETICAL AND EXPERIMENTAL BACKGROUND

Introduction

The interaction of the positron with matter has been studied since the experimental discovery of the positron in 1932. This chapter is a review of the work preceding the experiment which is the subject of this thesis. The experiment itself, fully described in later chapters, is only a part of the total effort being made to understand positron annihilation phenomena.

Free and Bound States of the Positron

Dirac (1) has calculated the cross section for annihilation of a free positron-electron pair, neglecting the Coulomb attraction between them. For non-relativistic velocities, this cross section is

$$\sigma = \pi r_0^2 c / v \tag{1}$$

where $r_0 = \frac{e^2}{mc^2}$ is the classical electron radius. The annihilation rate for this case is

$$R = \frac{1}{\tau} = \sigma v n \tag{2}$$

where τ is the mean life of the positron, and n is the free electron density. Then

$$\tau = (\pi r_0^2 c n)^{-1} \tag{3}$$

and

$$n = (N_0 \rho Z / A)\ cm.^{-3} \tag{4}$$

where N_0 is Avogadro's number, ρ is the mass density of the medium, Z the atomic number, and A the atomic weight. If all the electrons in a medium are assumed to be free,

$$\tau = (\pi r_0^2 c N_0 \rho Z/A)^{-1} = 2.2 \times 10^{-10} \left(\frac{A}{\rho Z}\right) sec. \tag{5}$$

The mean life is inversely proportional to the density, ρ, of the medium for free annihilation, and should vary from element to element.

Wheeler (2) used Equation (1) to obtain the lifetime of the positron in the singlet state of a bound system of electron and positron. This bound state, similar to an atom, was first suggested by Mohorovičić (3), and named positronium by Ruark (4). It can form in either the singlet state with spins antiparallel, or the triplet state with spins parallel. Since Equation (1) is an average over all spin possibilities, Wheeler first multiplied it by four, in order to deal with the singlet state alone. The singlet state decays with emission of two quanta, the triplet state decays to three quanta. The annihilation rate is given by

$$\frac{1}{{}^1\tau_{2\gamma}} = {}^1\sigma_{2\gamma} v |\psi(0)|^2 = 4\sigma_{2\gamma} v |\psi(0)|^2 \tag{6}$$

where ${}^1\tau_{2\gamma}$ is the singlet mean lifetime and $|\psi(0)|^2$ is the probability that a positron lies in a unit volume in the immediate neighborhood of the electron, and $\psi(0)$ is the ground state wave

function evaluated at a separation of zero between the particles. Wheeler then substituted $|\psi(0)|^2 = \frac{1}{8\pi a_0^3}$ where a_0 is the Bohr radius, and obtained

$$\frac{1}{{}^1\tau_{2\gamma}} = \left(4\pi\lambda_0^2 \frac{c}{\nu} \cdot \frac{\nu}{8\pi a_0^3}\right) = \frac{1}{2}\alpha^5 \frac{mc^2}{\hbar} \qquad (7)$$

where α is the fine structure constant. Numerically,

$${}^1\tau_{2\gamma} = 1.25 \times 10^{-10} \text{ second.} \qquad (8)$$

Annihilation of an electron - positron pair with the emission of three quanta was studied by Ore and Powell (5). They calculated

$$\frac{\sigma_{3\gamma}}{\sigma_{2\gamma}} \approx \frac{1}{370} \qquad (9)$$

for the ratio of cross sections, and applied the result to the ^3S ground state of positronium to obtain

$$\frac{{}^1\tau_{2\gamma}}{{}^3\tau_{3\gamma}} = \frac{1}{1115} \approx \frac{\alpha}{8} \qquad (10)$$

or

$${}^3\tau_{3\gamma} = 1.39 \times 10^{-7} \text{ second.} \qquad (11)$$

If positronium is formed, it will occur in the triplet state three times as frequently as in the singlet state. This increases the ratio of three quanta to two quanta processes above the value 1/370, with a maximum ratio of 3/4 possible.

Referring back to Equation (5), it should be noted that there is an important difference between annihilation in the free state and annihilation in the bound state. For positronium, the electron density n is not the mean density in the positronium atom. Thus the mean life of positronium against self-annihilation should not vary with the

density of the medium. Equation (5) gives mean lives of the order of 10^{-7} second in gases at atmospheric pressure, and mean lives of the order of 10^{-9} to 10^{-10} second in solids (6).

In order to show that the ^1S state cannot decay to an odd number of photons and the ^3S state cannot decay to an even number of photons, consider the operation of charge conjugation, as applied to an electron - positron pair (7). This operation changes the sign of the two particles, which is equivalent to reflecting the particles through the origin and exchanging their spins; i.e., parity times spin exchange. The states of positronium are required to be antisymmetrical with respect to space, spin, and charge coordinates of the two particles by the Pauli principle. Both singlet and triplet positronium have odd parity, but the singlet state is odd under spin exchange and is therefore even with respect to charge conjugation, while the triplet state is even under spin exchange and odd with respect to charge conjugation. The eigenvalue of the charge conjugation operator for states containing n photons is $(-1)^n$. The charge conjugation operator is a constant of motion, so the singlet state must annihilate into an even number of quanta and the triplet state must annihilate into an odd number of quanta (8).

All possible energy states of the bound electron - positron system, positronium, are reduced by a factor of two in comparison to the hydrogen atom due to the reduced mass of the system. The expression for the energy of the n^{th} state is thus

$$E_n = - \frac{e^4 m}{4\hbar^2 n^2} \quad . \tag{12}$$

The ionization potential is 6.8 volts and the ground state separation

of the two particles is twice that of the electron - proton distance in the hydrogen atom, 1.06 Å (9).

Annihilation in Gases

In order to study the mechanism of pair annihilation, Shearer and Deutsch (10) measured the mean lifetimes of positrons in several gases. Their measured values were of the order of 10^{-7} second, in agreement with theory, and decreased with increasing gas pressure. Gases were chosen so that the decay rate of free positrons would be slower, leading to longer and more easily measured mean lifetimes.

The work of Shearer and Deutsch (11,12) showed that the decay rate of positrons in gases is actually complex. Three separate lifetime components exist, as follows: a very short lived component, of the order of 10^{-10} second, due to the annihilation of parapositronium, a second lifetime of the order of magnitude to be expected from Equation (5), indicating the annihilation of free positrons, and a third lifetime of the order of 10^{-7} second, but independent of the pressure of the gas.

It was believed that this third component was due to the formation and annihilation of orthopositronium, since the measured lifetime agreed with the theoretical calculation of Ore and Powell (5). Deutsch proved this to be the case experimentally by introducing small amounts of nitric oxide, a gas consisting of molecules with an odd number of electrons, into the previously studied gases. This had the effect of rapidly converting the triplet state to the singlet state by electron exchange, thus greatly decreasing the triple coincidence rate.

The formation and stability of positronium can be discussed from the viewpoint of energetics (6,9). Upon entering a gas, the positrons undergo inelastic collisions with the gas molecules, slowing them down to energies below the first excited state of the gas molecules. This occurs in a time very short in comparison to τ as calculated from Equation (5). While the kinetic energy of the positron is greater than the ionization energy of the gas molecules, E_i, ionization by collisions is more probable than positronium formation. If positronium is formed, it is rapidly broken up again by collisions. This remains true for positron kinetic energies down to the first excitation level, E_1, of the gas molecules. Also, if the kinetic energy of the positron drops below the difference $(E_i - 6.8$ ev), where 6.8 ev is the binding energy of positronium, the positron has insufficient energy to capture an electron. If $E_1 > (E_i - 6.8)$, then there is a small range of energies, called the "Ore gap" for which positrons may form positronium. Figure 1 is an energy diagram depicting the Ore gap.

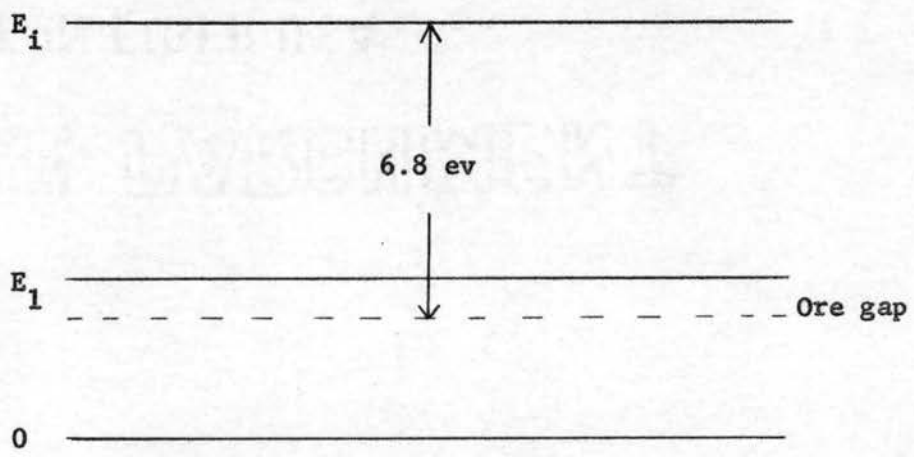

Figure 1. The Ore Gap.

Annihilation in Solids and Liquids

Lifetime measurements were extended to liquids and solids in the early 1950's, the most important investigation being carried out by Bell and Graham (13). They measured the absolute value of the positron lifetime in a variety of substances. A single lifetime of the order of 10^{-10} second, denoted by τ_1, was found for metals, apparently independent of the electron density of metals. In amorphous solids such as plastics, fused quartz and borax, and in water, they observed two lifetime components, one of the order of 10^{-10} second, the other of the order of 10^{-9} second. Their results also showed that the photons from the latter group of materials had the same energy as those from the metals, and that the radiation consisted mainly of pairs of photons strongly correlated at 180^{o} in both cases (14).

Subsequent measurements in solids and liquids led to two classifications of materials as regards positron annihilation in them. Grouped in one class are the τ_1 materials, such as metals and ionic crystals, which are characterized by the motion of free electrons throughout the crystal or crystallites. The materials in which the longer component also appears are placed in the second class. These are molecular materials with no attractive covalent forces between molecules (15). The question of regularity of structure, or crystallinity, does not enter into the classification of a material, since both classes have crystalline materials. Some polymers which are almost completely crystalline exhibit the long component.

The explanation proposed for the longer component, denoted by

τ_2, was that positrons, after slowing down in the sample, form triplet positronium in some fraction of the cases. The triplet positronium is then converted by some means to the singlet state, resulting in a lifetime shorter than that for the triplet state.

Thus a material exhibiting the longer lifetime component should yield more three quantum annihilations than one not showing it. Some triplet state atoms of positronium would decay by the emission of three quanta before conversion occurred. This conclusion was proven correct by Graham and Stewart (16) who found a low, constant three quantum rate for metals, and a higher rate for the amorphous materials, with the highest measured rate corresponding to the longest τ_2 component.

The mechanism which is now generally accepted as the one responsible for the depopulation of the triplet state and appearance of the τ_2 component is that of "pickoff" (17,18). In this process, the positron forms triplet positronium with an electron of the material, but then annihilates by two quantum emission with an electron of the proper spin orientation belonging to one of the surrounding atoms of the solid (19). The probability of pickoff depends on the amount of positron and electron wave function overlap, and therefore should also depend on the density of the material.

Some other explanations of the τ_2 component can be disposed of quickly. An exchange collision is possible in materials with atoms or molecules with unpaired electrons, but the τ_2 component appears in insulators, which have closed shells with paired electrons. Conversion from the triplet to the singlet state by spin flip through magnetic interaction takes about 10^{-5} second (15). Annihilation

from an excited state of positronium is not a plausible alternative either, since the excited states probably cannot exist in condensed materials. The binding energies of the 2s and 2p states are only about 1.7 ev (20).

The intensity of the τ_2 component, which is the percentage of positrons that annihilate by the pickoff mechanism, varies with the material. Values of this intensity, I_2, as low as 2% and as high as 51% have been measured (21).

The τ_1 component and its intensity I_1 are complex in nature for materials in which the positron decay is complex. They arise from annihilations of free positrons as well as singlet positronium. An estimate can be made as to how much each process contributes to I_1. Three of every four positrons in the bound state have spins aligned with their electrons. In the case of I_2, positronium is formed by all positrons contributing to I_2, or positronium is formed in a fraction 3/3 I_2 of cases. Singlet positronium is formed in a fraction 1/3 I_2. Then positronium, singlet and triplet, is formed in a fraction 4/3 I_2 of cases. For a substance in which $I_2 = 30\%$, $I_1 = 70\%$, singlet positronium is formed in a fraction 1/3 I_2, or 10%, so 1/7 of all short lifetime annihilations are attributable to singlet positronium (15).

The situation for metals and ionic crystals is explained in terms of nonformation of positronium. In metals the positrons quickly thermalize and are "swarmed" by the free electrons before positronium can be formed. The puzzling lifetime independence of the electron density was cleared away with improved equipment and techniques. Both Bell and Jørgenson (22) and Bisi et al. (23) have measured lifetimes

in metals that are density dependent. When the experimental annihilation rates (τ_1^{-1}) are plotted as a function of r_s, the dimensionless parameter which is the radius of the sphere whose volume equals the volume occupied by each valence electron in the metal, they lie on a smooth curve. Much theoretical work is being done presently to obtain a model which will fit the experimental curve. Equation (5) gives values of τ too long by about an order of magnitude because it does not take into account the "Coulomb enhancement" of the annihilating pair. Also, the mutual repulsion of electrons in the vicinity of the positron must considered.

Bell and Jørgenson also found evidence of a complex decay in metals, the slightly longer component being of low intensity, $\sim$ 5%. They could not explain their discovery since formation of positronium seems to be out of the question.

Ionic crystals can be considered to be constructed of tightly packed elastic spheres with radii of one to two angstroms. Most simply put, then, there is no room for the bound state in these materials. Positrons most likely annihilate with outer electrons of the negative ions, and the lifetime should therefore depend on the cube of the ionic radius.

An important point in the interpretation of positron lifetimes in solids is the thermalization time of positrons. In metals, for instance, positrons will be slowed down rapidly by collisions with electrons. Lee-Whiting (24) calculated a thermalization time of 3×10^{-12} second for metals, considerably shorter than the lifetime of positrons. Such calculations are not easy for insulators, but it seems probable that complete thermalization does not always take

place in them before annihilation, since positrons lose energy to the point where they are no longer able to excite electrons to a higher band. De Benedetti et al. (25) calculated 3×10^{-10} second for the thermalization time in gold due to excitation of lattice vibrations. This may be carried over as an indication of what the thermalization time may be in insulators.

The Temperature Effect

Bell and Graham also noticed a temperature effect in their measurements. The τ_2 component increased with increasing temperature of the material. In other words, the rate of annihilation decreases with increasing temperature, contrary to the direction of most physical processes.

The suggestion of pickoff led Wallace (20) to a simple explanation of the temperature effect. He assumed that positronium moves adiabatically in the nuclear potential, and is most probably found in the larger interstices, near the potential minima. Increasing the temperature of a material then induces greater molecular motion and larger molecular separations. In these enlarged intermolecular "holes", pickoff annihilation is less likely. So the temperature effect may also correctly be thought of as a density effect.

The effect of phase change on the τ_2 component is vividly seen in the measurements of Landes, Berko, and Zuchelli (26) on polycrystalline naphthalene. The crystalline regions of this material completely melt over a very small temperature region at about $80^{\circ}C$. The τ_2 component was constant at about 1.3×10^{-9} second from room temperature up to the melting temperature, and then took a jump upwards

to about 2.6×10^{-9} second at 80°C, above which it levelled off again.

Stump (27) has shown that the τ_2 component decreases with increasing pressure applied to a number of materials. De Zafra and Joyner (28), through their angular correlation studies, showed that decreasing the volume of a sample by applying mechanical pressure reduces the amount of positronium formed in it, and increasing the temperature increases the amount of positronium formed. Increasing and decreasing the volume available for positronium formation increases and decreases the positronium binding energy, respectively. This is equivalent to widening and narrowing the Ore gap in a material, which, providing the positrons are uniformly distributed in energy between 0 and E_i - 6.8 ev after their last inelastic collision, accounts for changes in amounts of positronium formed.

The Free Volume Theory

The preceding discussion of τ_2 and its variation with temperature or density has been of a qualitative nature. A theoretical expression for the τ_2 component as a function of the free volume of a material has been presented by Brandt, Berko, and Walker (29). The free volume is the average volume available to a positronium atom, and varies, as does density, with temperature. The complex structure of amorphous materials such as the polymers are a tremendous obstacle to any such theoretical procedure. Brandt roughly assumed that the positronium atom moves through a lattice of square potentials of height U_o, electron density ρ_o, and volume v_o, centered in a unit cell of volume v_1. The annihilation rate by pickoff which then

depends on the overlap of positronium with the lattice molecules is given by

$$\gamma_p = \pi r_0^2 c \rho_0 \int_{v_0} \psi^*_{Ps} \psi_{Ps} \, d^3 r . \tag{13}$$

This equation was evaluated in the Wigner - Seitz approximation, with the result

$$\gamma_p = \frac{\pi r_0^2 c \rho_0}{1 + F(U_0, r_0, r_1)} . \tag{14}$$

Then with the lifetime of free positrons in the medium expressed as

$$\tau_0 = (\pi r_0^2 c \rho_0)^{-1}$$

$$\tau_2 = \frac{1}{\gamma_p} = \tau_0 \left[1 + F(U_0, r_0, r_1) \right] \tag{15}$$

where r_0 and r_1 are the radii of volumes v_0 and v_1, respectively. The function F was evaluated and plotted as a function of v^*, the reduced cell volume v_1/v_0, for several different values of the scattering parameter $P_0 r_0^2$, where

$$P_0 r_0^2 = \left(\frac{4m}{\hbar^2} \right) U_0 r_0^2 .$$

This evaluation was carried out for three different kinds of lattice geometry; planar, hard-sphere, and cylindrical, the last of which is used in the case of polymers whose long molecules resemble cylinders. Now

$$\tau_2 = \tau_0 \left[1 + F(P_0 r_0^2, v^*) \right] . \tag{16}$$

With the knowledge that

$$v^*(T=0) = \frac{V_1(T=0)}{V_0} = \frac{2\sqrt{3}}{\pi} \tag{17}$$

for cylindrical geometry, $v_1(T=0)$ being the specific volume at $T=0^{\circ}K$, and some specific volume versus temperature data, τ_2 can be calculated for a given temperature.

Lifetime calculations were carried out by these authors and compared to experimental data for Teflon and glycerol in the temperature range 0 to $300^{\circ}K$, and for ice and water in the range 100° to $350^{\circ}K$. The theoretical fit is fairly good for the first two substances, but fails to correctly predict the variation across the ice to water transition.

Objective of the Experiment and the Usefulness of Positron Lifetime Measurements

In light of the small amount of data available on the temperature, or density, effect, it was felt that further investigations in that direction would be of value in the field of positron annihilation studies.

In recent years, room temperature measurements of positron lifetimes in an assortment of polymers have made it clear that there is nothing to be gained from a comparison of these values for the same polymer. Polymer samples of the same type manufactured by different firms have different properties. Such factors as density, degree of crystallinity, thermal history, age, and the various kinds of radiation that permeate a plastic sample may influence the value of the lifetime of positrons in the sample.

If, however, the variation of lifetime as a function of temperature (i.e. density, or some other related property of the polymer) in the polymer is measured with an exacting technique and under

unvarying conditions, then this variation should be comparable to that measured by other investigators for the same polymer, or to similar data as measured for other materials.

Three polymers were chosen with the objective of measuring the effect that varying their temperatures has on the formation and annihilation of positronium in them. Particularly, values of τ_2 and I_2 will be presented later for polystyrene, Lucite, and polyethylene (Marlex 50) in the temperature range -200°C to +150°C.

Two immediate uses for such data come to mind. The first is to check the measured data against known variations of gross properties of the materials with temperature; the second is to provide more data for the previously described free volume calculation theory. Additional data of this nature may lead eventually to a more refined theory which in turn might mean a clearer understanding of the internal structure of polymers. This data should also show the reaction of positronium to the kinds of phase transitions encountered in the polymers chosen for this study.

The usefulness of the positron as a means of studying the structure of materials is limited. Distortion of the lattice structure by the positron itself is the price that is paid for information received. It would seem that the greatest benefit to be gained from positron lifetime studies will come from the theoretical models devised to fit the experimental data. If these models enlarge and clarify our present knowledge and pictures of the internal structure of matter and at the same time correctly explain other existing phenomena, then the positron lifetime method will be worthwhile. Otherwise, information of the nature obtained in this experiment and

others like it will reveal more about what happens to the positron after entering the material than about the material itself.

CHAPTER II

THE ELECTRONIC APPARATUS

The Coincidence System

The most important elements of an experiment to measure the mean lifetime of positrons are (i) a source which will signal the creation or formation of a positron so as to provide a reference point in time with which the annihilation signal may be compared and (ii) an electronic clock which is turned on and off by these signals. The entire circuitry for such an experiment is generally called a "fast-slow" coincidence system. Figure 2 is a block diagram of the apparatus used in this experiment.

The isotope Na^{22} is a positron emitter and was used as the source in this study. The emission of a 1.28 Mev gamma ray follows the emission of each positron by a time short in comparison to the positron lifetime, and thus acts as the creation signal. The annihilation gammas have energy 0.51 Mev. The method of source deposition and the samples themselves are dealt with in the next chapter.

The gamma rays were detected by two scintillators and photomultiplier tubes. The scintillators used were Nuclear Enterprises NE 102 plastic cylinders, 1.5 inch in diameter and one inch long, in thin aluminum covers. The decay constant of these scintillators is 3.5×10^{-9} second. The aluminum covers fit tightly over the ends of

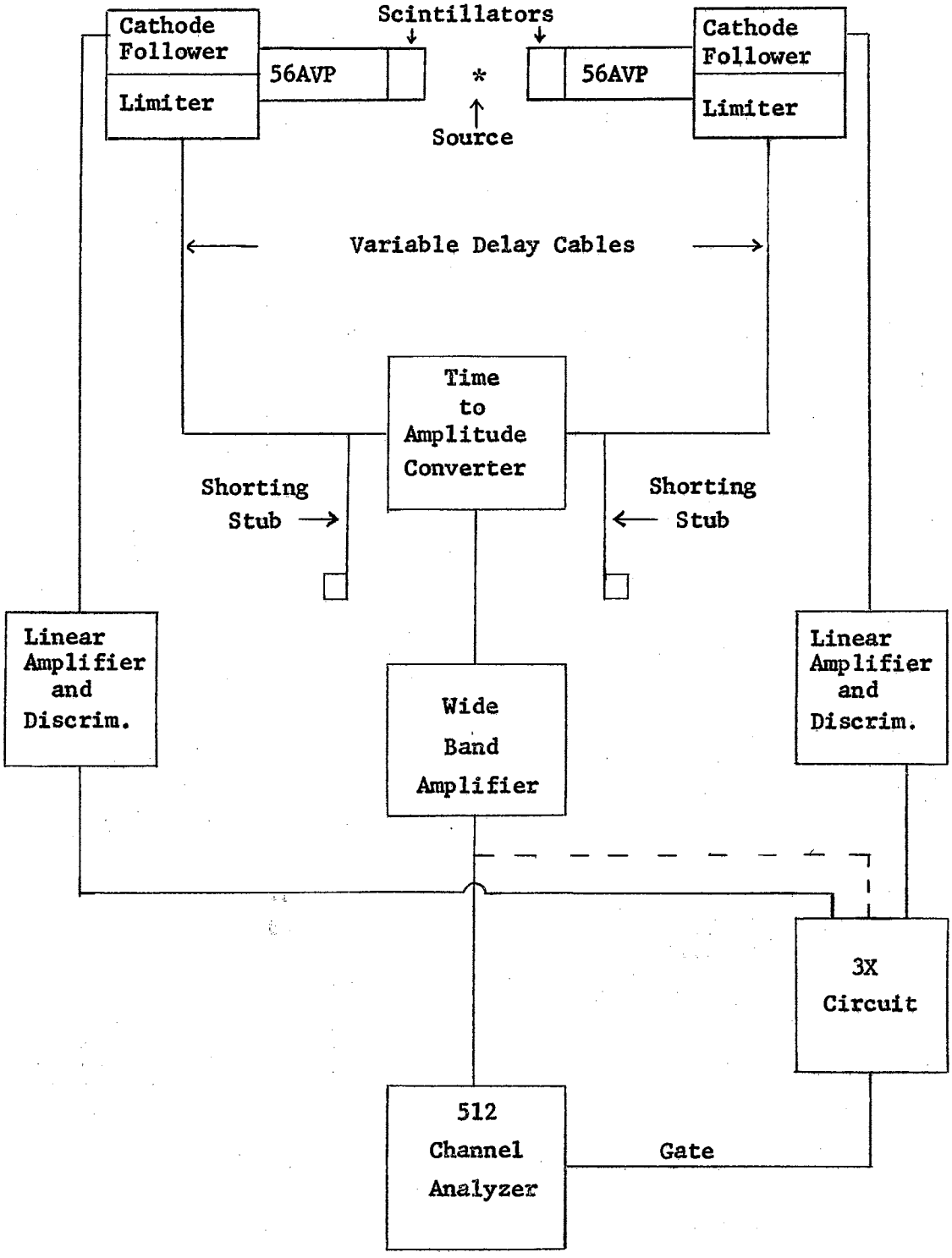

Figure 2

Block Diagram of the Apparatus

the photomultiplier tubes, and the scintillators were optically bonded to the photocathodes with Dow Corning silicon grease QC-2-0057. Amperex 56 AVP head-on fourteen stage photomultipliers were used. This tube was chosen because of its high gain (approximately 10^8 at 2000 volts), rapid rise time of output pulse (2×10^{-9} second, ideally), and short cathode time difference (3×10^{-10} second at 2000 volts).

The photomultiplier tubes were positioned horizontally at 180 degrees to each other, one being socketed in a fixed chassis, the other in a chassis that could slide back and forth along rails to facilitate sample changing. They were operated at 1850 volts, and were supplied by a Hamner Model N-4035 high voltage power supply. The AC line voltage for the entire system was regulated by a Sorensen Model 20008 voltage regulator.

Located in each chassis was a pulse limiter circuit and a simple cathode follower circuit. The limiter circuit consisted of a conducting pentode which was cut off by the large negative pulse from the anode of the photomultiplier. Western Electric 404-A and Amperex 5847 pentodes were used in the experiment. The resulting output pulse was a fast rising flat topped pulse, independent of the gamma ray energy. These pulses were transmitted by variable lengths of RG-7/U cable to T-junctions, where they split. Part of the limiter pulse flowed down a shorting stub of RG-8/U cable and was reflected at the short circuited end and returned to the T-junction. This reduced the width of the pulse to 2t, where t is the time required for the pulse to travel the length of the shorted RG-8/U cable. With 183 centimeter lengths of shorting stubs, 2t was about 18×10^{-9}

second. Thus only the fastest rising portion of the pulse was used.

The shorting stubs were connected directly to the electronic clock circuit, which is called a time to amplitude converter. This circuit, designed by Simms (30), is of the "overlap" type, with the height of the output pulse being proportional to the overlap in time of the two input pulses. Figure 3 shows the curcuit diagram of this instrument. All transistors are Western Electric 2N1195A. With no inputs, transistors T_1 and T_2 are conducting, and T_3 is cut off. If a positive pulse cuts off either T_1 or T_2, all the current I flowing through R_1 is carried by the other input transistor. If both transistors are cut off for a time Δt, i.e., a coincidence occurs, the current is switched into T_3 and integrated at the collector of that transistor. The amplitude of the output pulse is given by

$$V = I \Delta t / C_s \tag{18}$$

where C_s is the stray capacitance at the collector of T_3. For best conversion, both input pulses should have constant, equal amplitudes greater than 0.6 volt. It was noted throughout the experiment that room temperature changes caused fluctuations in the output pulse height.

The switching transistors T_1 and T_2 were balanced with the operating detectors. The bias on T_3 was reduced with the 10K potentiometer until single input pulses were observed at the output. By varying the 1K potentiometer, the amplitude of the output pulse was then made the same with either input cable removed. After T_1 and T_2 were balanced in this manner, the bias on T_3 was increased again until no single pulses were observed at the output. The purpose of

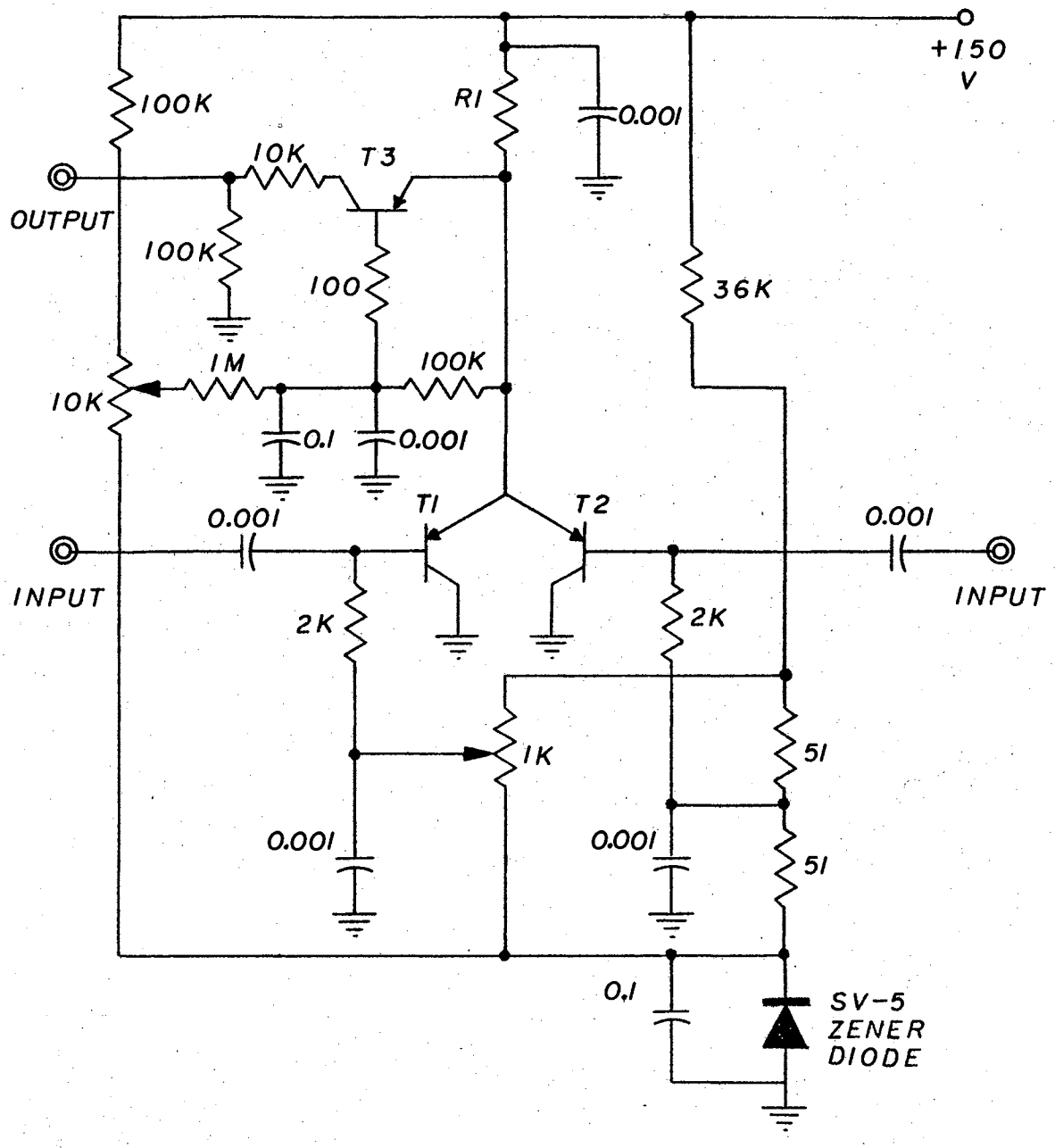

Figure 3

Circuit Diagram of the Time to Amplitude Converter

the 5 volt Zener diode is to raise the bases of the transistors above ground and provide collector voltage. Along with Simms, no difference in performance was noted due to soldering the transistors directly into the circuit over placing them in transistor sockets.

The positive output pulse of the time to amplitude converter was then transmitted to a Hewlett Packard Model 460BR wide band amplifier where it was inverted and further amplified. From this point, the pulses were fed to a Nuclear Data (Model ND 130) 512 Channel Data Analyzer. This equipment formed the "fast" part of the system, and set the time restrictions for the experiment.

It was also necessary to set energy restrictions for the detected gammas, and this was accomplished in the "slow" part of the circuit. Positive pulses from the cathode followers, which were connected directly to the tenth dynodes of the photomultipliers, were conveyed by RG-7/U cables to Baird Atomic Model 215 non-overloading amplifiers with discriminators. The discriminator of one amplifier was set to pass only those pulses representing the detection of 1.28 Mev gammas, and the other was set to pass both 0.51 Mev and 1.28 Mev pulses. This prevented false coincidences between two 0.51 Mev pulses.

The output pulses of these amplifiers were transmitted to an Advance Radiation Engineering Corporation Model 401 Coincidence - Anticoincidence Analyzer, which has a resolving time of one microsecond. If pulses from each amplifier arrive at this coincidence circuit within one microsecond of each other, a positive pulse approximately four microseconds wide appears at the output. This pulse served as a "gate pulse" for the 512 channel analyzer; that is, it opened or turned the analyzer on to allow it to count the time to amplitude

converter pulses. Thus a pulse from the time to amplitude converter had to represent a true coincidence in order to be counted, a true coincidence being one that satisfied both the time and energy conditions of the circuit.

The most important component of the analyzer is an analog-to-digital converter which produces, in response to each input pulse, a number (called the channel number) whose magnitude is a linear function of the peak amplitude of the input pulse. The analyzer also has an internal linear amplifier for additional amplification of input pulses.

Calibration

The data spectrum stored in the memory of the analyzer could be displayed on an oscilloscope, where it appeared as a plot of logarithm of coincidence counts on the ordinate versus channel number on the abscissa. The data were also read out digitally on an IBM electronic typewriter. It was desirable to convert the abscissa to a time scale in order to calculate lifetimes; this was done by calibrating the time to amplitude converter. The calibration was carried out by inserting different lengths of delay cable between one of the limiter circuits and the converter, and recording the peak channel (or more properly the centroid) of the time distribution curve for a source of "prompt" gammas. A plot of delay length or time delay inserted in one detector channel versus peak channel exhibited a linear region except for total overlap and very small overlap of input pulses. Figure 4 is such a calibration curve for the apparatus used in this experiment. The reciprocal of the slope of the linear region gives a

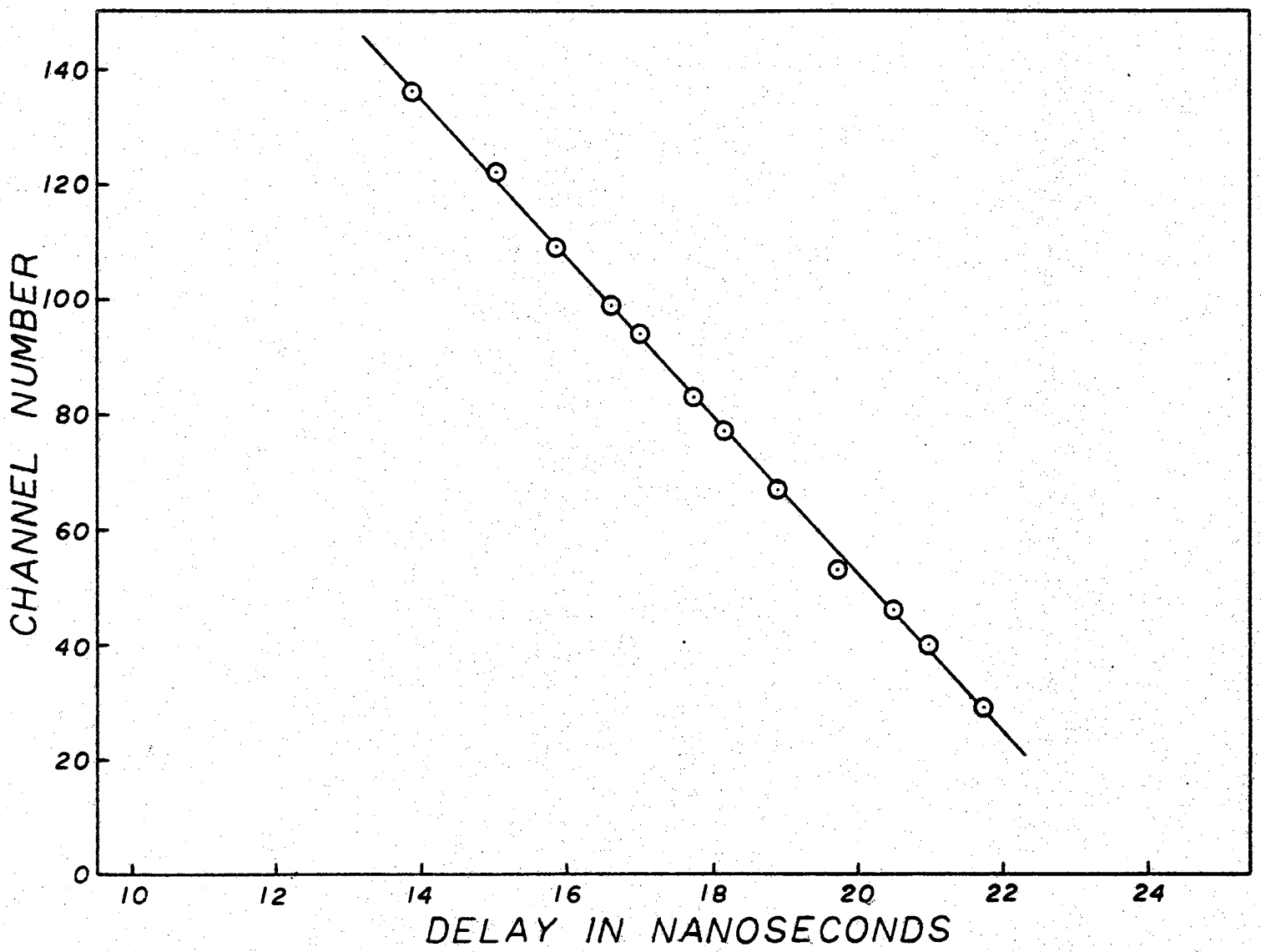

Figure 4

Apparatus Calibration Curve

calibration constant in units of time per channel. The calibration constant was 0.0727×10^{-9} second/channel throughout most of the experiment, with an approximately 9 nanosecond range of linearity.

The source of "prompt" gammas may actually be one with a delay between emitted gammas which is short compared to the resolving time of the apparatus. An example is the annihilation of positrons in aluminum, for which the time distribution curve is an inverted bell shape, indicating a single mean lifetime for the positrons. It differs from the time distribution curve of a true prompt source, such as cobalt 60, only in that the centroid of the aluminum curve is shifted in time from the true zero position of the apparatus by an amount equal to the lifetime of positrons in aluminum. The value accepted for this lifetime throughout the experiment was 1.9×10^{-10} second, as determined by Bell and Jørgenson (22).

The calibration of the time to amplitude converter is the limiting factor in the accuracy of experimental lifetime measurements. The time standard for calibration, which may vary by several per cent, is the velocity of a signal in the particular type of coaxial cable used. Cables may deteriorate with age and further uncertainties arise from connectors and attenuation of the signal in the cables (31). The numerical error estimated for the calibration constant, which is reflected in the numerical errors of the lifetimes, will be discussed in Chapter 4.

The resolving time of the apparatus is defined as the width of the prompt curve at half-maximum. It is a measure of the precision with which the electronic arrangement can determine the true time interval between events. It should not be confused with the coinci-

dence resolving time of the time to amplitude converter, but in fact it depends on the various sources of time spread in the detector and the coincidence resolving time. For the aluminum curves used as the prompt curves in this experiment, the resolving time was 7.9×10^{-10} second. Figure 5 is an example of two such time distribution curves for positron annihilation in aluminum taken with different time delays.

Ideally, the shapes of these curves would be triangles with slopes equal to the decay rate of positrons in aluminum (32). They are broadened due mostly to three sources of time fluctuations in the detectors. These sources are (i) duration of the scintillation, (ii) the time required for the scintillation light to reach the photocathode, which depends on the distance traversed, and (iii) transit time, the time between the formation of a photoelectron and the arrival of the electron avalanche at the anode. Fluctuations in transit time arise principally from differences in path length (31).

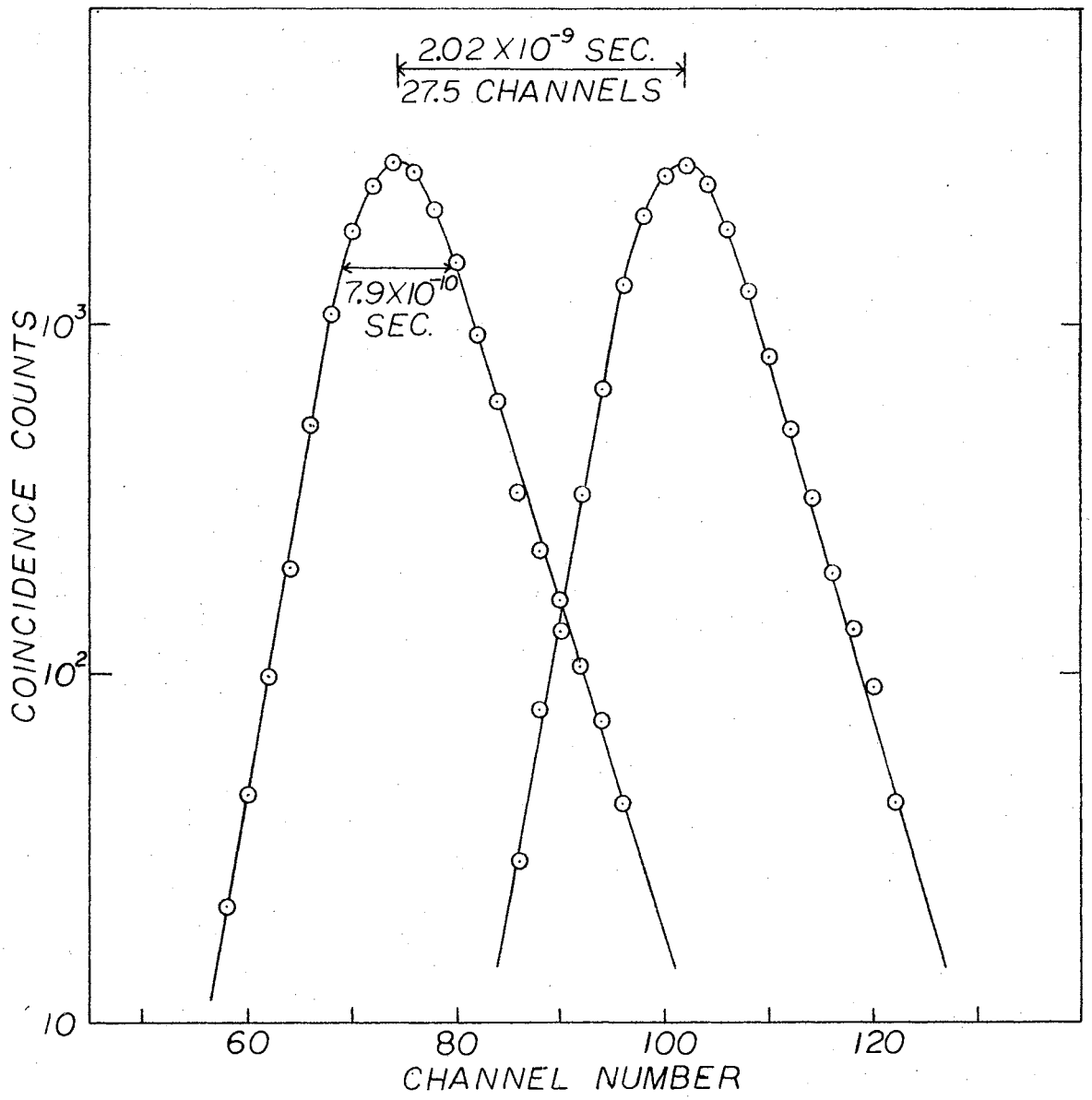

Figure 5

Aluminum Time Resolution Curves

CHAPTER III

THE SAMPLES

High and Low Temperature Apparatus

The method of depositing the source of positrons directly on the plastic samples was found to be the most satisfactory for this experiment. Plastic samples cylindrical in shape were made as shown in Figure 6. Small holes for thermocouple wires were also drilled into the sample.

Approximately ten microcuries of Na^{22} was deposited in the "well" of one half of the sample. The other section of the sample made a force fit into the well. This isotope, having a half life of 2.6 years, decays in 89 per cent of the cases by positron emission to an excited state of Ne^{22}. The samples were of sufficient thickness that no positrons could escape, and no annihilations could take place except in the sample and the source itself.

Katz and Penfold (33) in a review of electron range - energy studies, proposed the empirical relation

$$R_0(mg/cm^2) = 412 E^n \qquad (19)$$

$$n = 1.265 - 0.0954 \ln E$$

for the effective maximum penetration depth for electron energies E in the range 0.01 Mev to 3 Mev. This relation may be applied to

positrons since the maximum annihilation cross section for them occurs only at relatively low energies, and they behave like electrons during most of the slowing-down process. The maximum penetration depth R_m for a continuous energy spectrum with maximum energy E_m is the same as the above R_o for monoenergetic electrons. Taking E = 0.5 Mev, the maximum positron kinetic energy for the decay of Na^{22}, R_o is 164 mg/cm^2. The maximum penetration depth is then $d = R_o/\rho$. Marlex is the least dense of the samples, having $\rho = 0.96 \times 10^3$ mg/cm^3, so d = 0.171 cm. As seen from Figure 6, the thickness of the wall of the well is 0.100 inch or 0.254 cm., considerably greater than the maximum penetration depth. It is estimated that less than one per cent of the annihilations could take place in the source.

Temperatures above room temperature were achieved by ohmic heating of a copper rod provided with a cylindrical hole to hold the plastic samples.

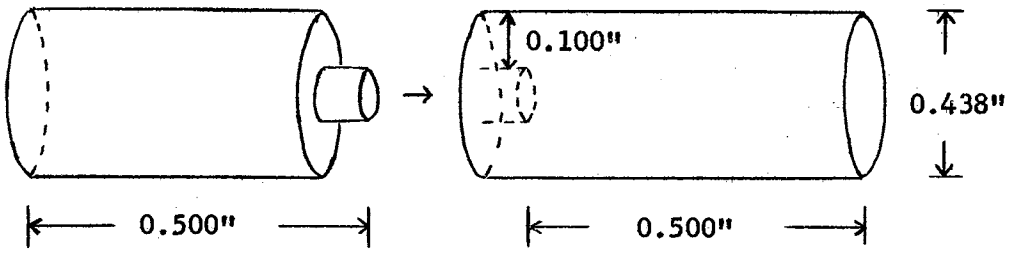

Figure 6

Shape and Dimensions of the Plastic Samples

The rod was approximately twenty inches long and one inch in diameter. A hole 0.500 inch in diameter was drilled completely through the rod, halfway between the ends. This hole accommodated copper cans with outside diameters of 0.500 inch, in which the cylindrical samples were placed. The purpose of the cans was to keep the plastics from clogging the hole when they flowed and to prevent contamination of the rod due to diffusion of the source at higher temperatures.

Three feet of 26 gauge Chromel heating wire was wrapped in coils five and one-half inches long, one and one-half inches on each side of the hole, forming two coils which were connected in parallel to a regulated direct current voltage supply. Sauereisen cement insulated the wire from the rod. The entire rod was wrapped with asbestos tape to insulate against thermal radiation.

Temperature regulation was accomplished with a Minneapolis - Honeywell Model No. 105C204P Pyr - O - Vane Millivoltmeter controller. Its sensor is a calibrated copper-constantan thermocouple, and it is capable of regulating to $\pm 0.5^{\circ}C$ in the range $-200^{\circ}C$ to $+300^{\circ}C$.

Two holes were drilled in the top of each plastic sample, about 0.070 inch on each side of the center. Into one of these was inserted the regulator thermocouple, and into the other another thermocouple connected to a Leeds and Northrup K-2 potentiometer with standard cell and galvanometer. This equipment was used to more accurately measure the temperature and the magnitude of the temperature variation.

The maximum variation was $\pm 0.5^{\circ}C$, which occured only at the higher temperatures. If there was any temperature gradient across the sample, it was less than $0.5^{\circ}C$, and undetectable.

The rod was placed horizontally between the detectors, with the plastic sample carefully centered between them. This method allowed equal heating of the entire sample, excellent regulation, and small, controlled increases in temperature when desired.

A disadvantage of the method was heating of the scintillators, and possible heating of the photocathode. Changing the temperature of the scintillator changes its decay time, and increased temperature increases thermal emission from the photocathode. In order to guard against these, an additional brass cap was placed over each scintillator such that there was about an eighth of an inch between the face of the scintillator and the end of the cap. The end of the cap was made very thin (0.060 inch) to minimize stopping of gamma rays, and each cap had two nozzles so that water or air could be run through them to cool the scintillators. Also, the caps were not put in direct contact with the rod.

The low temperature data were obtained by placing the cylindrical plastic samples in a dewar flask with a narrow flange at the bottom. The samples rested on the bottom of the flange, and cooling mixtures were poured into the dewar. The flange, and particularly the sample, was then centered between the detectors.

The low temperatures obtained and mixtures used were; $0^{\circ}C$, ice and water; $-13^{\circ}C$, methyl alcohol and ice; $-78.5^{\circ}C$, dry ice and methyl alcohol; $-124.6^{\circ}C$, methyl alcohol and liquid nitrogen; $-196.0^{\circ}C$, liquid nitrogen. Data were also obtained at $-28.0^{\circ}C$, by placing the samples in one end of a metal sample holder, the other end of which was extended into a dewar containing dry ice and methyl alcohol.

Properties of the Samples

A description of the physical properties of polymers in general, and the three sample materials used in this experiment in particular, is now in order.

Polymers, or plastics, consist of long chain molecules, made up of repetitive monomer units. The arrangement of these molecules in the polymer may be both crystalline and amorphous. No polymer is either completely crystalline or completely amorphous; there are regions of both states throughout the polymer. The long chain molecules pass through both regions, the length of the crystalline regions being a few hundred angstroms. The crystalline state is characterized by regularity and order of structure, all the chain molecules being parallel. A definite unit cell of particular geometry may be assigned, and the inter-molecular spacing may be determined by x-ray diffraction methods (34).

The amorphous state is characterized by complete disorder, the molecules having random orientations, with the possibility of large inter-molecular "holes". To a distance of about 15 Å from any point in the structure, the spatial arrangement of amorphous polymers and those of simple liquids or organic glasses are very similar (35).

Polymers are capable of undergoing two types of phase transitions. The first, called a first-order transition, is due to the complete melting of all crystallites, and is identified by the crystalline melting point, T_m, at which discontinuous changes in density, heat capacity, and transparency occur. At this temperature the material becomes a viscous liquid (34,36).

The second-order transition is associated with the amorphous regions of polymers, and is identified by the glass transition temperature T_g, at which discontinuous changes in specific volume and thermal expansion occur. At temperatures above T_g, there is segmental motion of the linear polymer molecules due to thermal energy and to the existence of free volume. Below T_g, the free volume becomes smaller and the thermal energy kT becomes small compared to the potential energy barrier heights for rotational and translational jumps of the polymer segments. The polymer molecules are restricted to vibrational motions about equilibrium positions (34,35). In appearance, the polymer is a hard glassy material below T_g, and a soft rubbery material above T_g.

The glass transition has a somewhat lesser effect on polymers with a high degree of crystallinity than on those that are almost completely amorphous. It is the only detectable transition that occurs in the latter.

Polystyrene, $[CH_2CHC_6H_5]_n$ and Lucite, or polymethyle methacrylate, $[CH_3CH_2C(OCOCH_3)]_n$, are both almost completely amorphous. A plot of specific volume versus temperature for polystyrene shows a small linear decrease in volume with temperature below T_g due to contraction of the lattice. Above T_g the relation is also linear, but with a greater slope. The intersection of these two straight lines with positive slopes is the glass transition temperature, T_g (36,37). The slopes of these lines are roughly in the same proportion as the coefficients of expansion of the polymer above and below T_g. These are $2.5 \times 10^{-4}/C^{o}$ below T_g, and $5.5 \times 10^{-4}/C^{o}$ above T_g (35). The actual temperature at which the glass transition occurs depends on the rate of heating of the sample, but is generally located between

80° and 100°C.

The shape of the volume versus temperature curve for Lucite is the same as for polystyrene. The coefficients of expansion are $1.95 \times 10^{-4}/C^{\circ}$ below T_g, and $5.0 \times 10^{-4}/C^{\circ}$ above T_g. The glass transition probably occurs between 60° and 80°C (35,36).

The Marlex 50 polyethylene, $(C_2H_4)_n$, manufactured by Phillips Petroleum Company, is 85 to 93% crystalline, as measured by x-ray diffraction and nuclear magnetic resonance (38,39). The unit cell of Marlex 50 is orthorhombic with a = 7.41 Å, b = 4.94 Å, and c = 2.53 Å at 30°C, "a" and "b" being interchain distances, and "c" the chain repeat distance (34,40,41). (See Figure 7.) The changes in these dimensions with temperature have been studied by Swan (41) and Holmes (42). The "a" dimension shows a non-linear increase from 7.15 Å at -196°C, through 7.41 Å at 30°C, up to 7.71 Å at +138°C. The "b" dimension, on the other hand, changes from 4.90 Å at -196°C to only 4.94 Å at 30°C, and remains practically constant thereafter up to +138°C. The "c" dimension changes little or not at all over this entire temperature range.

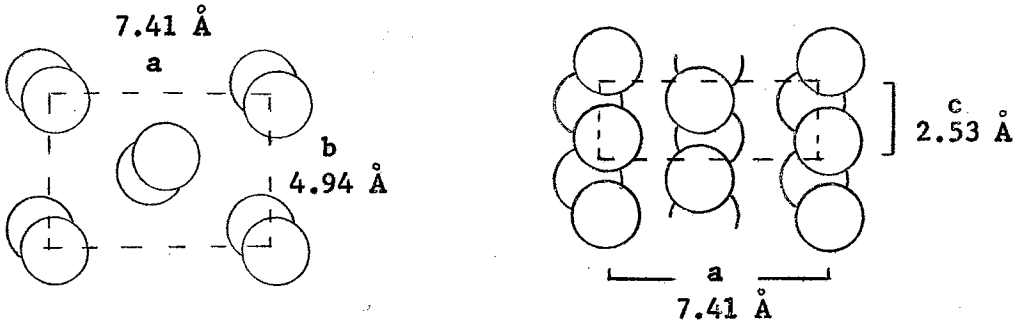

Figure 7 Polyethylene Structure

The specific volume of Marlex 50 shows a non-linear increase with temperature from -196°C to just below the crystalline melting point, and then a sharp rise to a discontinuity at T_m. Above T_m, the specific volume increases linearly with temperature (43,44,45). This relation is actually a composite of the crystalline and amorphous specific volumes, and the total specific volume, V, at any temperature is given by $V = XV_c + (1 - X)V_a$, where V_c and V_a are the specific volumes of the crystalline and amorphous phases, and X is the mass fraction in the crystalline phase. The V_c may be found from a knowledge of a,b, and c, and V_a may be found from a linear extrapolation to room temperature of the liquid specific volume measured in the region above the melting point. The melting point occurs in the range 130° to 140°C (41) and most of the crystallite melting is said to take place over a few degrees.

Although the specific volume varies smoothly with temperature up to T_m according to the previously quoted authors, there is evidence for a second order transition in Marlex 50 in the neighborhood of -20°C. Danusso, et al. (46), report a mean T_g of -21°C in Marlex 50 by dilatometric methods. Ohlberg and Fenstermaker (47) measured interchain separation as a function of temperature and obtained two straight lines intersecting at -28°C for polyethylene.

CHAPTER IV

PROCEDURE AND RESULTS

Temperature Procedure

At least two samples of a particular plastic were cut from the same piece of plastic. One was used for the high temperatures exclusively, data being taken as the temperature of the sample was increased from room temperature, 26°C, to above the melting point. The other sample was reserved for the low temperatures, data being taken as the temperature of the sample was decreased from room temperature to -196°C. There was no noticeable effect on the lifetime at room temperature due to the three different geometries; i.e., sample in rod, sample in dewar, sample alone directly between the detectors. This procedure was somewhat different than that followed by other authors (48,49), who have used one sample over an entire temperature range containing one or more phase transitions, or more than one sample, but in long overlapping temperature ranges, starting at lower temperatures. The reason for the procedure followed in this experiment is that the effect of temperature extremes on the properties of polymers is uncertain, and by arriving at these extremes at the end of data taking for that particular sample, and in doing so gradually, the effect on the lifetimes is minimized.

The time taken to increase the temperature of a sample ten to

twenty degrees was usually about two hours, although the increase was not always uniform. The temperature was maintained constant for data taking at least 24 hours. Sample temperatures were maintained even during equipment failures so that a consistent technique could be carried out. Great care had to be taken when cooling a sample to -196°C to avoid thermal shock, even if the sample had been at about -125°C previously.

Data Reduction

Experimental time distribution curves are a composite of the apparatus resolution curve and the coincidence curves due to the annihilation of positrons in the samples.

The basic equation for delayed coincidence experiments (50) is given by the integral

$$F(x) = \int_{-\infty}^{+\infty} f(t)\, P(x-t)\, dt \qquad (20)$$

where x is the inserted time delay, F(x) is the coincidence curve for the source whose decay time is to be measured, P(x) is the "prompt" curve, the coincidence curve for a source of simultaneous events, and f(t)dt in this case is the probability that a 0.51 Mev gamma will be emitted t seconds after a 1.28 Mev gamma. In these polymers, f(t) has two components.

The curve obtained for positrons annihilating in aluminum, after being corrected for the lifetime in aluminum, was used as the P(x) curve. For $F(x) >> P(x)$, the tail of the coincidence curve for the polymers approaches an exponential; i.e., positronium decays exponentially as do radioactive atoms. The decay constant can be deter-

mined by fitting a straight line through a semilog plot of the experimental points in this tail by a weighted least squares method (51). The slope of this line, or the decay constant, is given by

$$\lambda = \frac{\sum_i N_i (X_i - \bar{X})(Y_i - \bar{Y})}{\sum_i N_i (X_i - \bar{X})^2} \tag{21}$$

where N_i is the number of coincidence counts in channel x_i, y is ln N_i, and

$$\bar{X} = \frac{\sum_i N_i X_i}{\sum_i N_i} \qquad \bar{Y} = \frac{\sum_i N_i Y_i}{\sum_i N_i} .$$

Then the mean lifetime of positrons in the material is

$$\tau_2 = \frac{k}{\lambda} \tag{22}$$

where k is the calibration constant. (See Appendices A and B.)

Time distribution curves were allowed to accumulate until their shapes were well defined and there were sufficient counts in the tail region to obtain statistically good values of τ_2. The data were then typed out on an IBM electronic typewriter. From three to ten determinations of τ_2 were made for each sample at each temperature.

The determination of background, which must be subtracted from each data run, is extremely important in measurements of this nature. The background is due primarily to accidental coincidences, and to a lesser extent to outside events and higher - order coincidence pulses. Accidentals are due to the counting of 0.51 Mev and 1.28 Mev pulses not related to the same positron. Higher - order coincidences occur when a proper time reference pulse is counted in one channel or arm of the coincidence apparatus, but in the other channel a true coin-

cidence pulse is defective in amplitude and is rejected by the amplitude discriminator. If in this other channel a third pulse occurs within the resolution time of the triple coincidence system which is of proper amplitude to be accepted by the amplitude discriminator in that channel, but not necessarily a true coincidence event, it will open the pulse - height analyzer gate also.

Approximately nine nanoseconds of delay cable was inserted in one pulse channel, and the accidental coincidences were counted for from 30 minutes to 90 minutes. An average number of background counts per channel per minute was computed. This number times the counting time of a data run was subtracted from the number of counts in each channel of the data run. At least one background check was made for every three data runs at each temperature. The peak count rate - to - background ratio was better than 1200 to 1.

After subtraction of background, the data were plotted on semilog paper. Fifty consecutive points in the tail region of the time distribution curves for the polymers were used in Equation (21) to determine τ_2. The variance for each τ_2,

$$V_{\tau} = \frac{(1/\lambda)^4}{\sum_i N_i (x_i - \bar{x})^2} \tag{23}$$

was also determined. The statistical uncertainty in τ_2 is given by the square root of v_r times k, the calibration constant. Equations (21), (22), and (23) were programmed for IBM 650 and 1620 digital computers.

Aluminum time distribution curves were taken frequently. These were important for checking the electronic stability and in the

calculation of I_2, to be discussed later.

The most probable value of τ_2 and its uncertainty was found for each sample at each temperature. For a number of data runs, each run yielding a lifetime and uncertainty of $A_i \pm a_i$, the most probable value of lifetime and uncertainty (52) is

$$\bar{A} = \sum_i \frac{1}{a_i^2} A_i \Big/ \sum_i \frac{1}{a_i^2} \qquad \bar{a} = \sqrt{1 \Big/ \sum_i \frac{1}{a_i^2}} \,. \tag{24}$$

No attempt was made to determine the shorter τ_1 value for the polymers.

The intensity I_2 of the τ_2 component was calculated following the method of Green and Bell (21). It has the advantage of being much quicker than an alternate method, the "folding out" or centroid shift process (53), which was used in previous work (54). The centroid of the prompt curve is shifted to the right of the true zero of time of the coincidence circuit by an amount equal to the lifetime of positrons in aluminum, 1.9×10^{-10} second (22). The centroid of the prompt curve was obtained by dividing the net moments about an arbitrary point under the curve by the area under the curve. From this was subtracted the lifetime in aluminum, and the true zero was thus obtained. The straight line obtained from the weighted least squares fit to points in the tail was then extrapolated back to the true zero point. The area under this straight line divided by the area under the entire curve, multiplied by a correction factor, is the intensity I_2. The correction factor is required because of the finite width of the prompt curve compared with the value of τ_2. This correction is analogous to the correction for finite duration

of the counting interval when a repidly decaying source is being counted, and is given by $(\tau_0/\tau_2)[\sinh(\tau_0/\tau_2)]^{-1}$ where τ_0 is the half width at half height of the prompt resolution curve. This factor was about 0.95 in all cases. All areas were obtained by Simpson's rule. Figure 8 shows the τ_2 area (shaded) for a typically shaped time distribution curve.

Presentation of Results

Tables I, II, and III present the results for polystyrene, Lucite, and Marlex 50, respectively. They list temperature, most probable value of τ_2, and I_2, along with their errors.

Figures 9, 10, and 11 show time distribution curves of positron annihilation in polystyrene, Lucite, and Marlex 50, respectively, for the three different temperatures indicated on the figures. The number of coincidence counts in each channel along the curves is not shown, but only some representative points. The vertical lines show the standard deviation of the points, when it is greater than

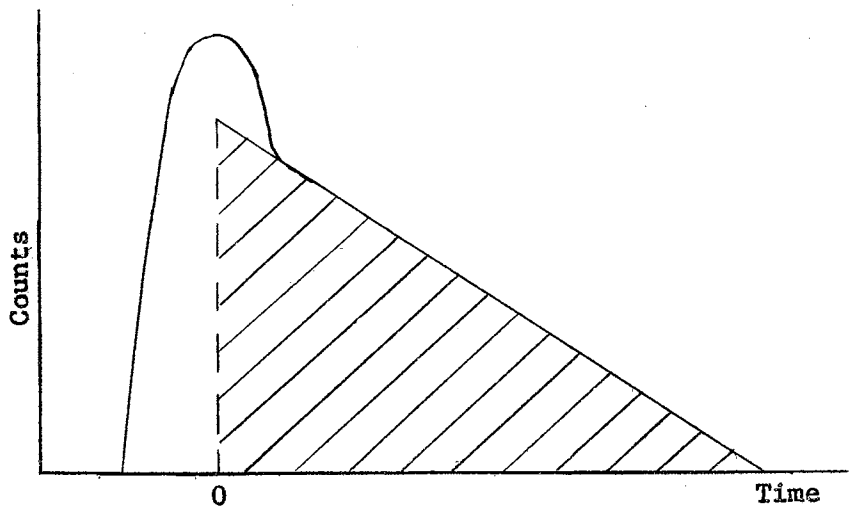

Figure 8 Area Associated With τ_2 Component

TABLE I

MEAN LIVES AND INTENSITIES IN POLYSTYRENE

Temperature in Centigrade Degrees	$\tau_2 \times 10^9$ Second	Intensity, I_2, in %.
147.6 ± 0.5	2.77 ± 0.08	32 ± 5
127.2 ± 0.5	2.59 ± 0.06	31 ± 5
108.0 ± 0.5	2.52 ± 0.06	32 ± 5
98.8 ± 0.5	2.46 ± 0.05	31 ± 5
84.0 ± 0.5	2.21 ± 0.05	30 ± 5
72.0 ± 0.3	2.14 ± 0.04	30 ± 5
60.8 ± 0.3	2.18 ± 0.05	32 ± 5
50.0 ± 0.2	2.07 ± 0.05	29 ± 5
39.5 ± 0.2	2.06 ± 0.05	31 ± 5
26.0	2.11 ± 0.05	27 ± 5
0.5 ± 0.5	2.13 ± 0.05	26 ± 5
- 13.0 ± 0.5	2.10 ± 0.04	22 ± 5
- 28.0 ± 2.0	2.07 ± 0.04	22 ± 5
- 78.5 ± 0.5	2.00 ± 0.04	20 ± 5
-124.6 ± 2.0	1.92 ± 0.05	21 ± 5
-196.5 ± 0.5	1.72 ± 0.05	19 ± 5

TABLE II

MEAN LIVES AND INTENSITIES IN LUCITE

Temperature in Centigrade Degrees	$\tau_2 \times 10^9$ Second	Intensity, I_2, in %.
126.0 ± 0.5	2.35 ± 0.07	21 ± 5
119.0 ± 0.5	2.31 ± 0.07	22 ± 5
112.5 ± 0.5	2.25 ± 0.07	22 ± 5
102.4 ± 0.5	2.21 ± 0.06	20 ± 5
93.1 ± 0.5	2.14 ± 0.05	20 ± 5
80.8 ± 0.4	2.11 ± 0.06	18 ± 5
71.6 ± 0.4	2.01 ± 0.06	20 ± 5
61.2 ± 0.2	2.06 ± 0.06	20 ± 5
51.7 ± 0.3	1.96 ± 0.06	21 ± 5
41.2 ± 0.2	1.99 ± 0.06	18 ± 5
32.8 ± 0.2	1.95 ± 0.05	20 ± 5
26.0	1.91 ± 0.04	19 ± 5
0.5 ± 0.5	1.94 ± 0.04	15 ± 5
- 13.0 ± 0.5	1.91 ± 0.04	15 ± 5
- 28.0 ± 2.0	1.95 ± 0.06	15 ± 5
- 78.5 ± 0.5	1.79 ± 0.04	15 ± 5
-124.6 ± 2.0	1.77 ± 0.06	17 ± 5
-196.5 ± 0.5	1.62 ± 0.04	14 ± 5

TABLE III

MEAN LIVES AND INTENSITIES IN MARLEX 50

Temperature in Centigrade Degrees	$\tau_2 \times 10^9$ Second	Intensity, I_2, in %
152.5 ± 0.5	3.25 ± 0.10	24 ± 5
142.3 ± 0.4	3.39 ± 0.12	28 ± 5
136.8 ± 0.4	3.23 ± 0.12	30 ± 5
128.2 ± 0.4	3.18 ± 0.09	25 ± 5
119.4 ± 0.4	3.05 ± 0.10	24 ± 5
102.7 ± 0.3	2.78 ± 0.11	25 ± 5
90.9 ± 0.4	2.80 ± 0.10	23 ± 5
82.2 ± 0.4	2.62 ± 0.06	21 ± 5
70.5 ± 0.4	2.48 ± 0.05	23 ± 5
59.5 ± 0.3	2.41 ± 0.06	21 ± 5
48.6 ± 0.3	2.33 ± 0.07	20 ± 5
39.6 ± 0.3	2.42 ± 0.05	18 ± 5
26.0	2.32 ± 0.04	19 ± 5
0.5 ± 0.5	2.21 ± 0.04	16 ± 5
- 13.0 ± 0.5	2.17 ± 0.05	14 ± 5
- 28.0 ± 2.0	1.90 ± 0.06	13 ± 5
- 78.5 ± 0.5	1.60 ± 0.04	12 ± 5
-124.6 ± 2.0	1.47 ± 0.06	13 ± 5
-196.5 ± 0.5	1.26 ± 0.04	11 ± 5

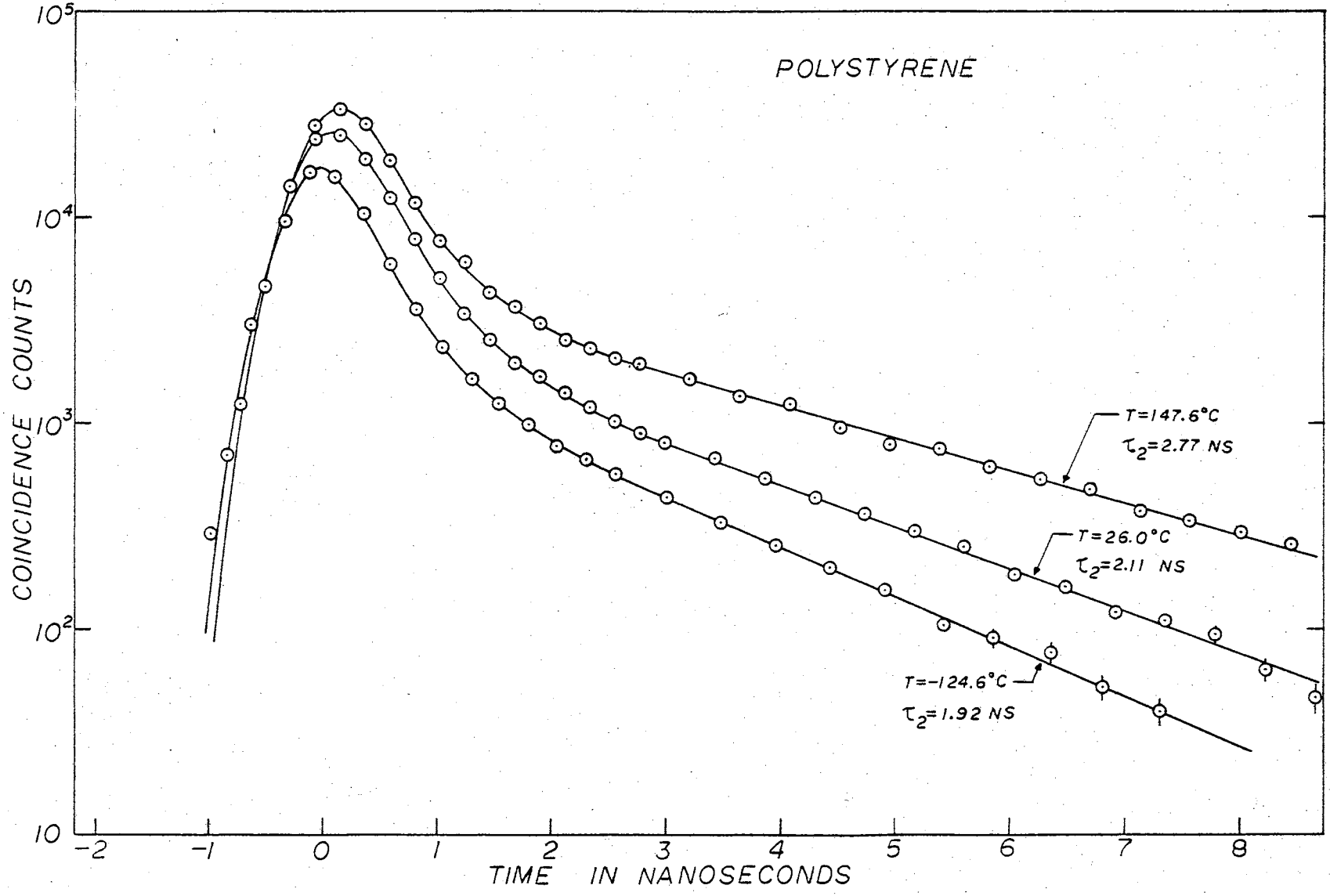

Figure 9

Time Distribution Curves for Positron Annihilation in Polystyrene

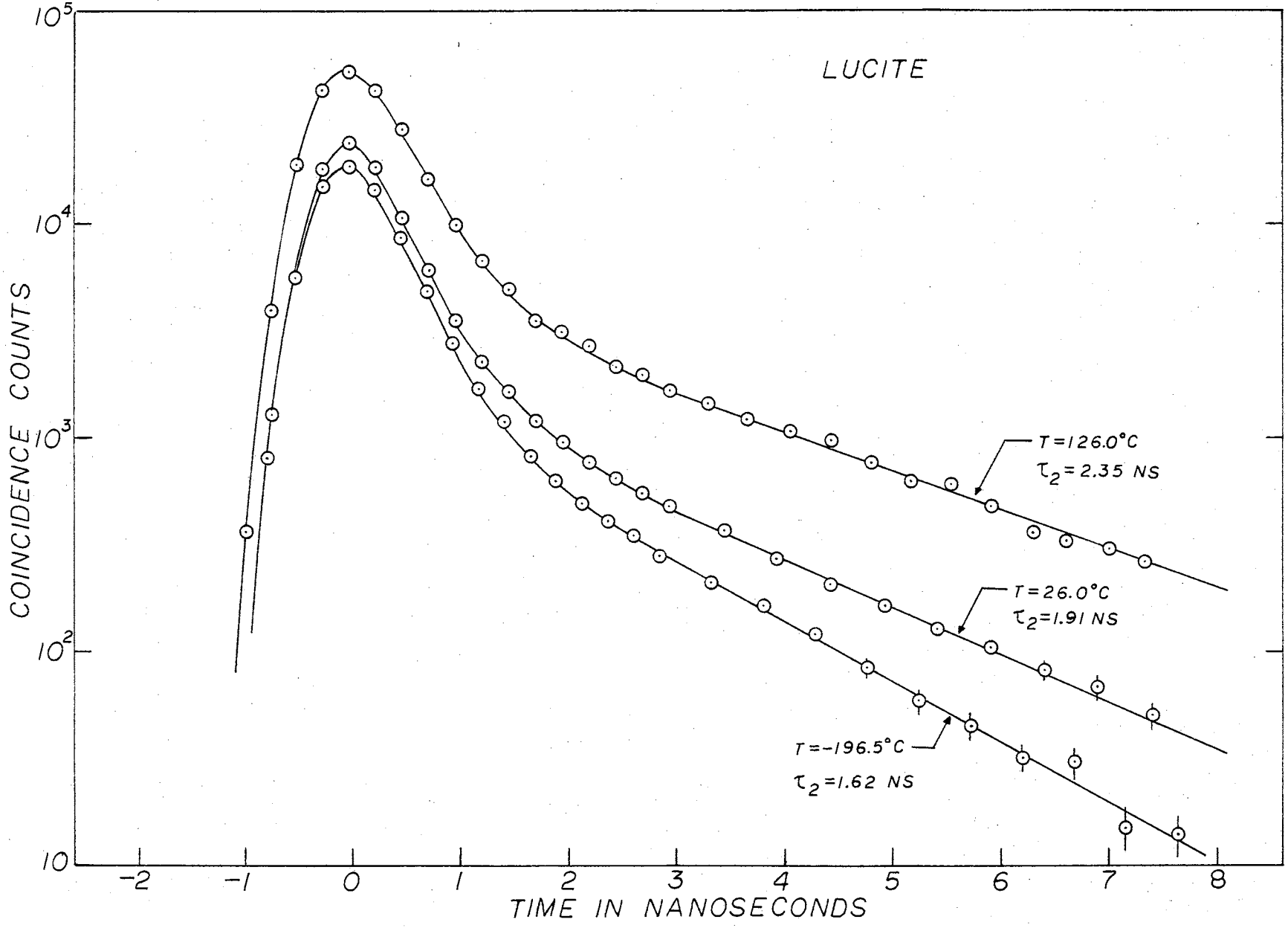

Figure 10

Time Distribution Curves for Positron Annihilation in Lucite

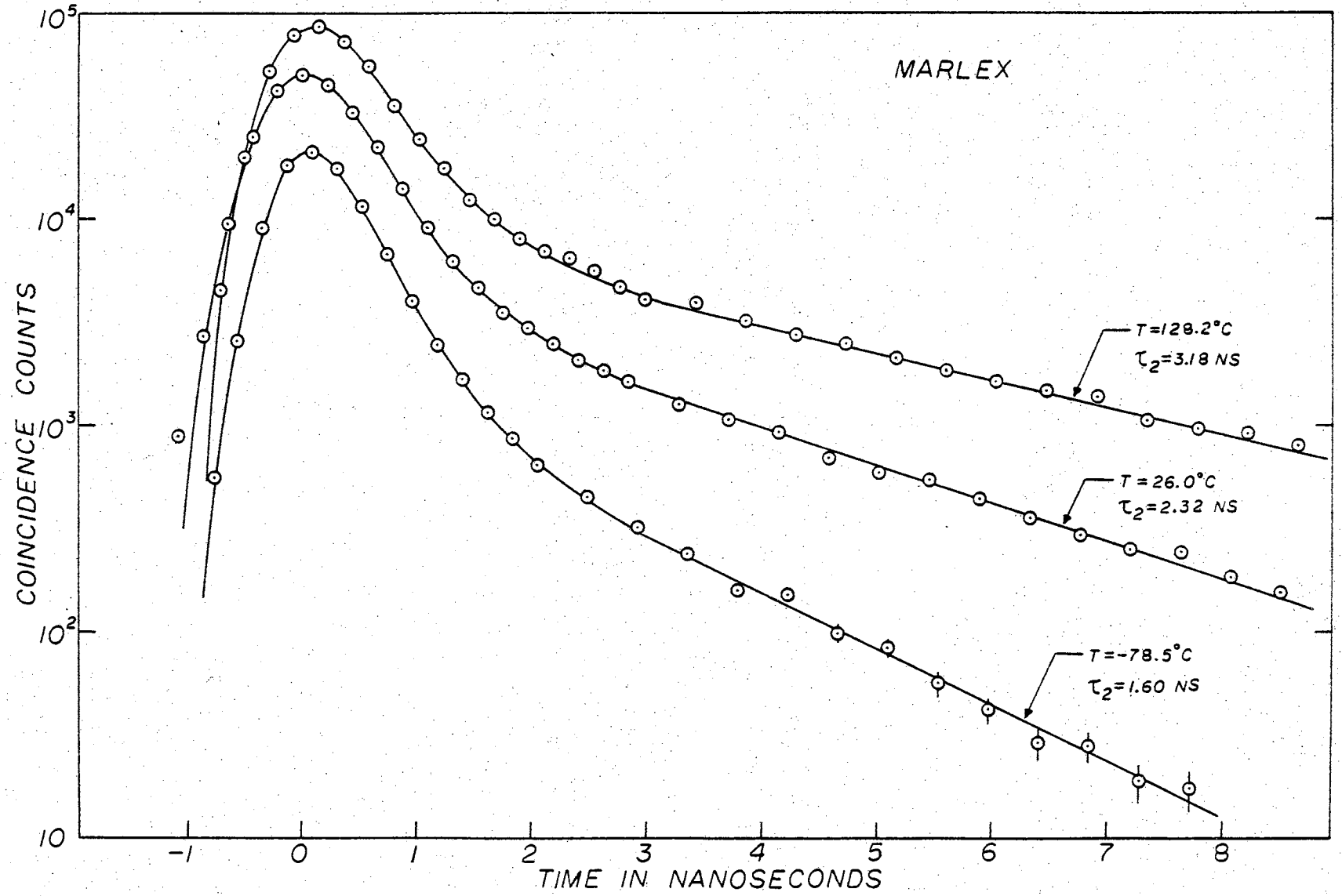

Figure 11

Time Distribution Curves for Positron Annihilation in Marlex 50

the radius of the small circle surrounding the points. All these curves show a pronounced two component decay.

Figure 12 shows the time distribution curve of positron annihilation in graphite at 26°C. A single mean life is present, with the value of $\tau_1 = 2.8 \pm 0.9 \times 10^{-10}$ second. The decay in this material was found to remain simple up to 100°C.

Some other data of interest concerned the mean life and intensity in two other samples of polyethylene, produced by Cadillac Plastics. One was a high density sample, with $\rho = 0.953$ gm/cm^3, the other of low density, with $\rho = 0.918$ gm/cm^3 (55). The purpose of taking this data was to show that differently prepared samples of the same polymer will yield different results in an experiment of this type. The results are summarized in Table IV. All data were taken at room temperature only.

TABLE IV

RESULTS FOR POLYETHYLENE SAMPLES

Sample	Most Prob. τ_2 (ns.)	I_2 (%)
low density polyethylene	2.47 ± 0.05	22 ± 5
high density polyethylene	2.18 ± 0.06	19 ± 5

Errors

The error quoted for τ_2 in the tables is due to three factors: (i) the statistical error in the determination of the calibration constant, k, (ii) the statistical error in determining the slope of

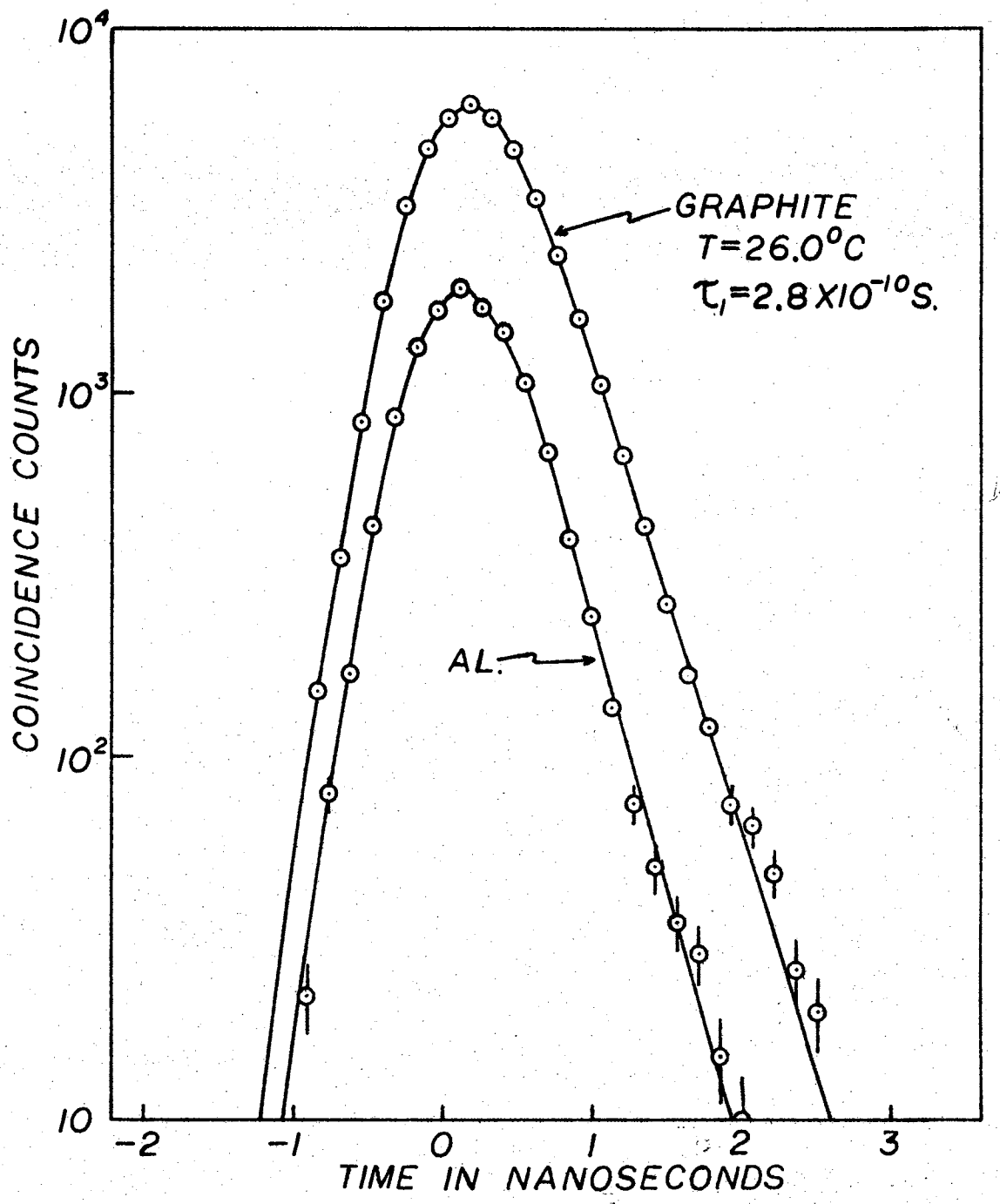

Figure 12

Time Distribution of Positron Annihilation in Graphite and Aluminum at 26.0°C.

the straight line fit to points in the tails of time distribution curves, as expressed by Equation (22), and (iii) systematic error, which includes background subtraction.

The first two of these are completely determinate and can be combined to give a total statistical error. The third is probably indeterminate and is best represented by an estimated amount which can be added to the statistical error.

Even with the assumption of rather generous deviations in cable length (or delay time), the error in k, determined by finding the standard deviation of the slope of the calibration curve, was a maximum of $\pm$ 0.01 nanosecond. The two statistical errors were considered independent, and combined by taking the square root of the sum of their squares.

An estimated systematic error of $\pm$ 0.02 nanosecond was added to the statistical error in τ_2. Determination and subtraction of background contributes strongly to the systematic error, but may be in one direction only. That is, too much or too little background is always subtracted.

The error quoted for I_2 in the tables is due to three factors: (i) the statistical error in finding the centroid of the resolution curve and the statistical error in the slope of the tail, (ii) instrumental drift due to temperature and voltage fluctuations occurring between a data run with a polymer sample and a data run with aluminum, and (iii) the approximate method by which the areas are found to compute I_2.

The standard error in the centroid, $\bar{x}$, is given by

$$(\sigma_{\bar{x}})^2 = \frac{\sum_i N_i (x_i - \bar{x})^2}{(\sum_i N_i)^2} \qquad (25)$$

where N_i is the number of coincidence counts in channel x_i (31). The error in I_2 due to the error in the slope τ_2 can be found by drawing lines with the maximum and minimum slopes, and recalculating I_2. The combination of these two errors does not amount to more than $\pm$ 1%.

Postulating a drift of $\pm$ 2 channels, and thereby an error of the same amount in location of the true zero, leads to an error in I_2 of $\pm$ 2%. This amount of drift is rather large for the data taking times in this experiment, thus the error quoted for this cause is an upper limit.

Finally, another 2% was added as an estimate of the uncertainty introduced by the Simpson's rule method of calculating areas. This uncertainty decreases somewhat with smaller intervals of calculation along the curve defining the area to be determined.

CHAPTER V

DISCUSSION AND INTERPRETATION

Introduction

The experimental results are explained in terms of the shape of τ_2 versus temperature plots, and changes in free volume in the materials caused by changes in temperature.

The free volume per gram, v_f, is $v_1 - v_o$, where v_1 is the specific volume and v_o the excluded volume per gram, which may be found from Equation (17) in Chapter I. The specific volume, of course, is the gross, macroscopic volume per unit mass of the sample. The percentage of the total volume that is free at any temperature T is given by $\frac{V_1(T) - V_o}{V_1(T)} \times 100\%$. This percentage at room temperature was calculated to be 16% for polystyrene, 16% for Lucite, and 17% for Marlex, in rough agreement with the estimate of 20% for polymeric materials based on compressibility data (56)

The free volume as defined above is also called the empty volume (57), and differs from two other definitions of free volume sometimes used in regard to polymers or liquids, the expansion volume and the fluctuation volume. The expansion volume (per unit mass) at any temperature is the specific volume at that temperature less the specific volume at $0^{\circ}K$. The fluctuation volume is the volume swept out by the centers of gravity of the molecules as a result of their

thermal vibration. It is the empty volume, which will continue to be called the free volume, which is the most pertinent of these quantities to the formation of positronium.

Discussion of Plots

The mean life data of Tables I, II, and III were plotted as a function of temperature, and appear in Figures 13, 14, and 15. The vertical lines connected to the experimental points in these plots represent the error in τ_2.

The experimental lifetime points for polystyrene from -196.5°C to +84.0°C were fit with a straight line of slope 1.39×10^{-3} nanosecond/C°, and the points from 84.0°C to 147.6°C were fit with another straight line of slope 7.86×10^{-3} nanosecond/C°. The 84.0°C point was included on both lines because polystyrene began to get soft at about this temperature. The two straight lines intersect at 75.0°C, however. The ratio of the slopes of these lines is 5.66, which is larger than the ratio (2.20) of the volume expansion coefficient above T_g to that below T_g, as quoted by Tobolsky (35).

In Figure 14, the experimental lifetime points for Lucite from -196.5°C to +71.6°C were fit with a straight line of slope 1.35×10^{-3} nanosecond/C°, and the points from 71.6°C to 126.0°C were fit with another straight line of slope 5.91×10^{-3} nanosecond/C°. The temperature at which these lines intersect, 71°C, agrees with the glass transition temperature for Lucite observed by Robinson, et al. (58). The ratio of slopes is 4.38, and is larger than the ratio of volume expansion coefficients, 2.57 (35).

Although no direct correlation can be made between per cent

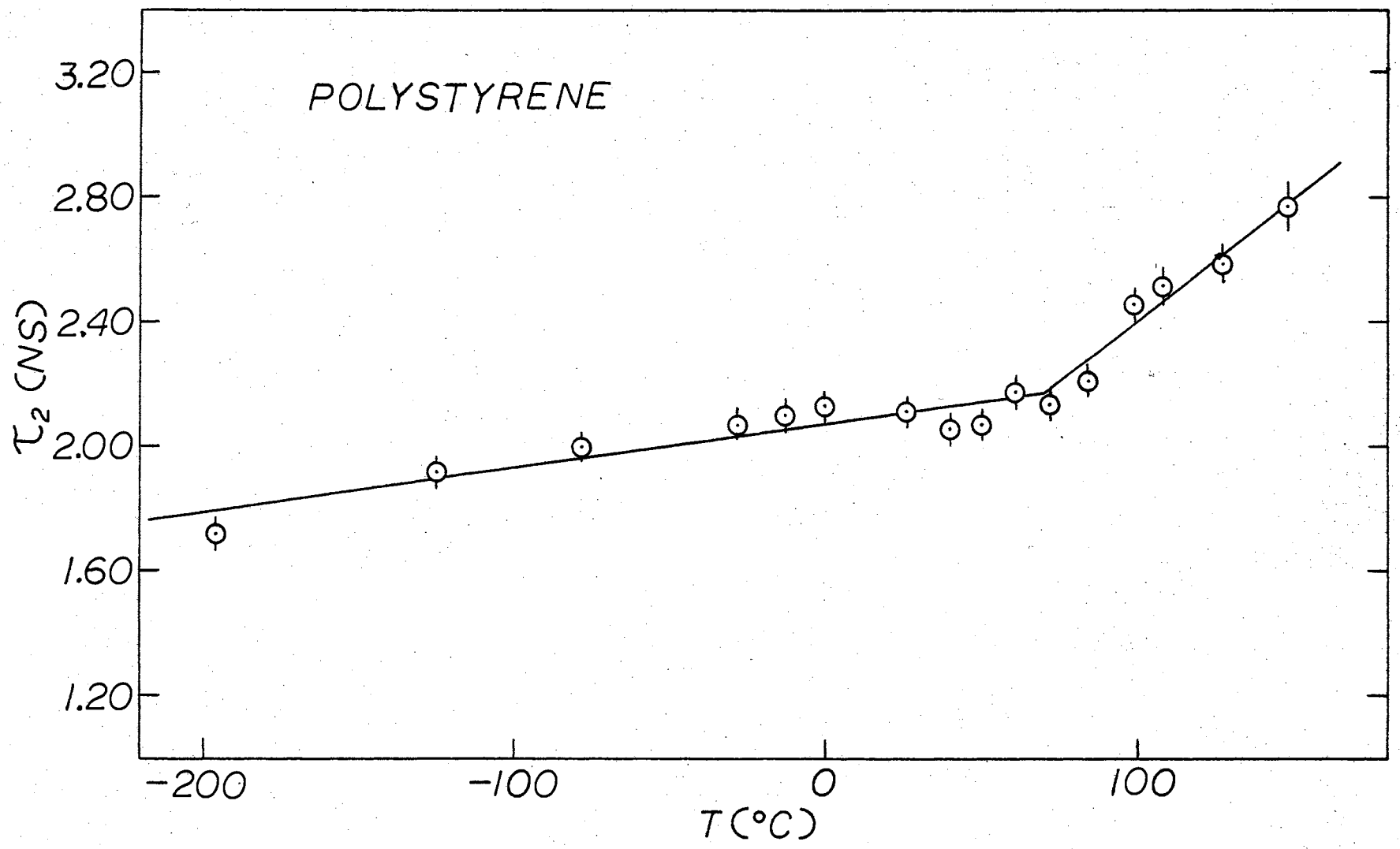

Figure 13

Experimental Mean Life (τ_2) Versus Temperature in Polystyrene

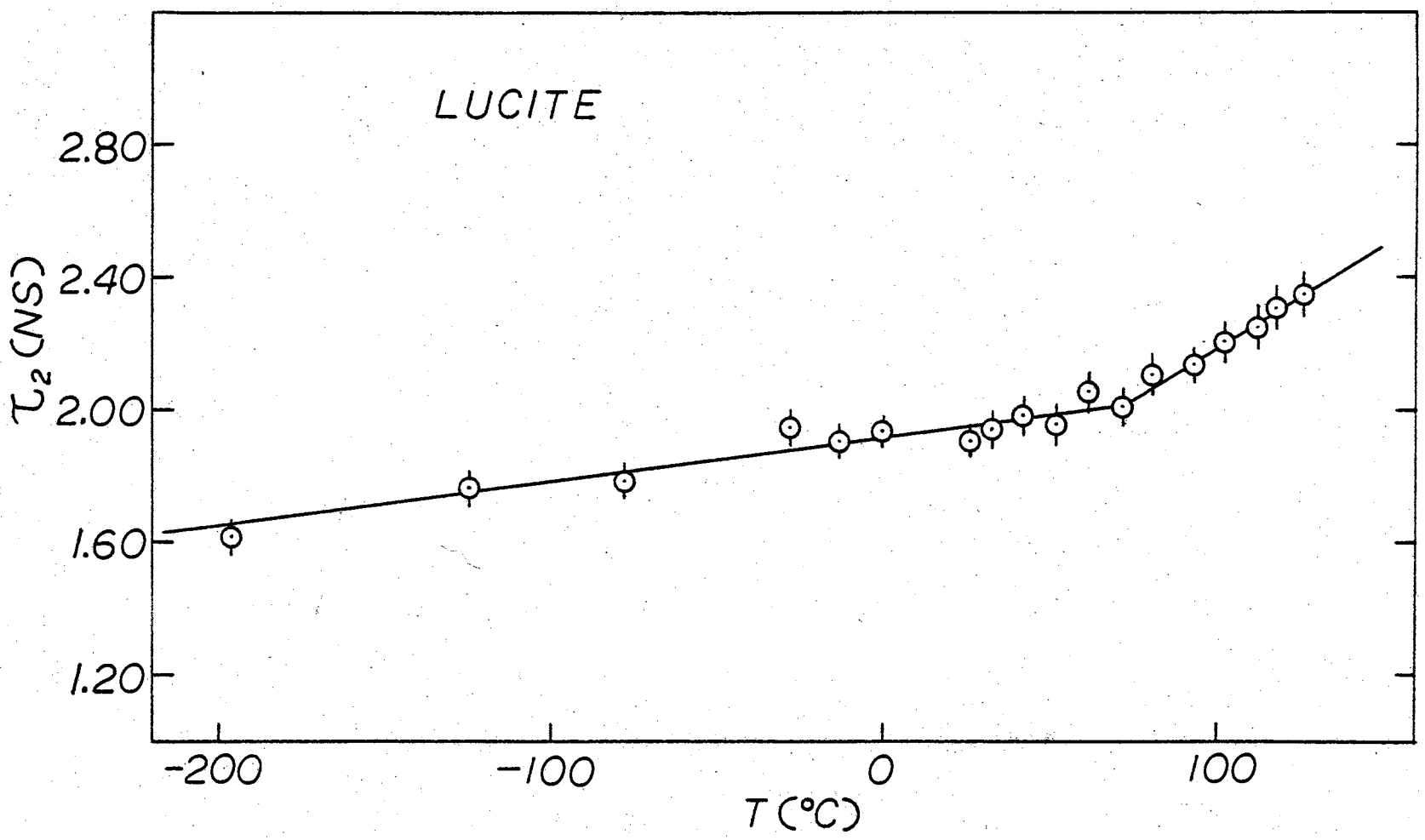

Figure 14

Experimental Mean Life (τ_2) Versus Temperature in Lucite

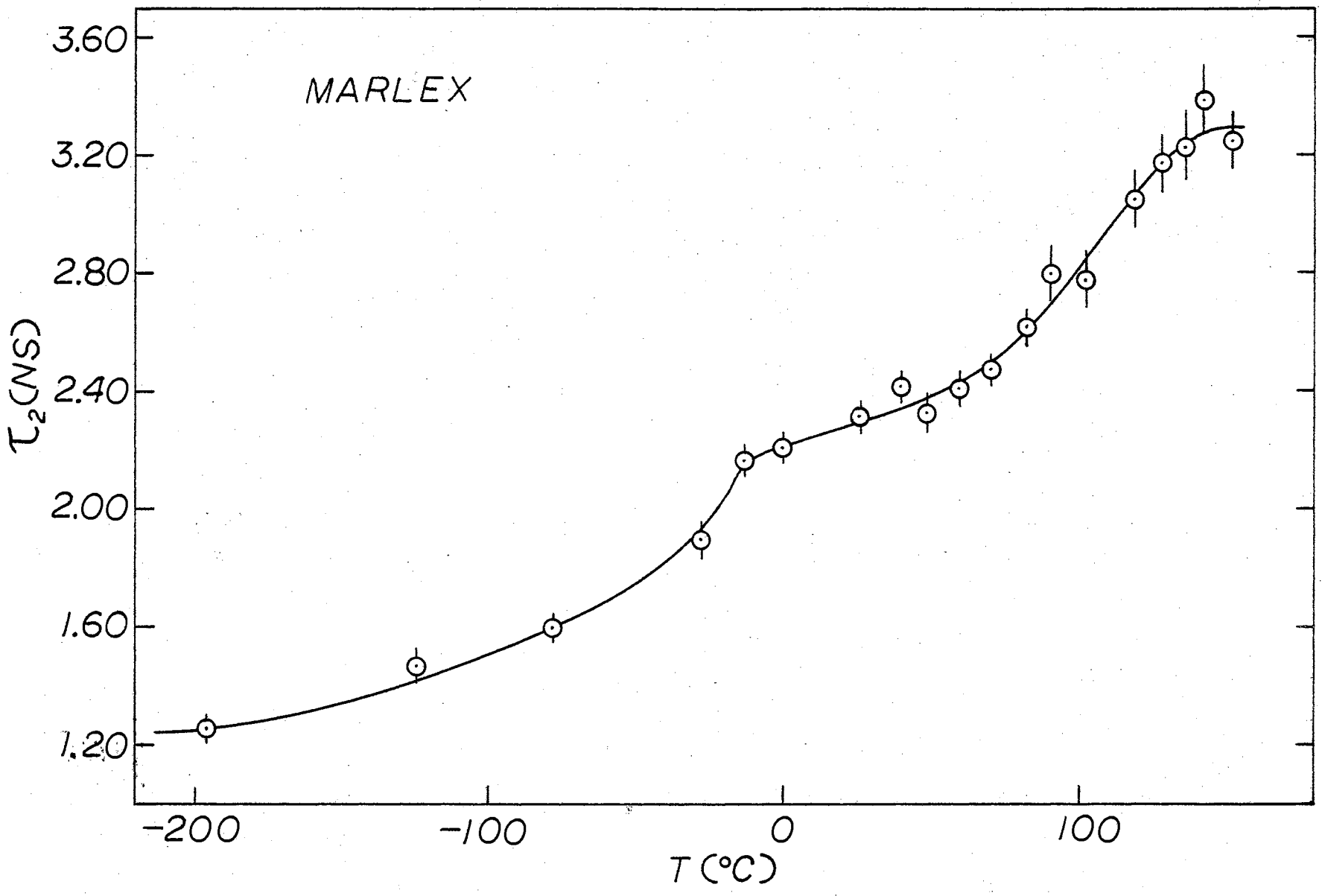

Figure 15

Experimental Mean Life (τ_2) Versus Temperature in Marlex 50

increase in τ_2 and per cent increase in free volume over any temperature range in these two polymers, it is satisfying that the data may be represented by two intersecting straight lines in both cases, resembling the specific or free volume variation of these substances described in Chapter III. It seems reasonable to state that the temperature effect is basically a free volume phenomenon in polystyrene and Lucite. The positron annihilation method has been shown in this experiment to be sensitive to glass transitions in polymeric materials.

The data for polyethylene are not so easily explained. A line which visually seemed to fit the points best was drawn. For temperature increasing from 26°C the lifetime gradually increases, and seems to level off at about 140°C. The sample melted at 131°C. The shape of the curve in this region resembles the specific volume versus temperature curve described for polyethylene earlier, but there is no sharp rise. Below 26°C there is a sudden and perhaps discontinuous change in the neighborhood of -20°C. This is the region in which a second - order or glass transition has been reported, but the shape of the lifetime curve does not resemble those for polystyrene and Lucite at their glass transition temperatures. Two possible explanations are tendered: (i) According to most data, the small change in density at this temperature would not account for the change in lifetime, but perhaps a lattice transition, such as occurs in Teflon (49) at room temperature might be responsible. (ii) A partially crystalline polymer that has been oriented by stretching exhibits an expansion parallel to the direction of orientation greater in magnitude than the expansion normal to the direction of orientation at T_g (59). This

expansion cannot be represented by the usual intersection of two straight lines at T_g, but rather is a sharply increasing function of temperature at T_g which levels off above that temperature.

The first suggestion seems to be ruled out on the grounds that all low temperature x-ray diffraction measurements of unit cell dimensions show no great or discontinuous changes. The "a" dimension in Marlex is still about 7.3 A at -20°C. There seems to be no reason to assume a "closing up" of crystalline regions to positronium. The transition at -20°C should be associated with the amorphous regions of the polymer in any case.

If the sample of Marlex was stretched during preparation, the variation at -20°C might be the reaction of positronium to the expansion parallel to the direction of orientation, with the expansion normal to the direction being masked.

Unfortunately there is no lifetime data across low temperature transitions in polymers with which to compare this data. The slow increase of τ_2 with temperature above 26°C indicates the slow melting of the crystalline regions, and presents a different behavior than that noted by Landes (26) in naphthalene which melts completely over a two or three degree interval with a consequent sharp rise in τ_2. There was no disappearance of the τ_2 component at low temperatures in any of the samples.

Theoretical Calculations

Theoretical free volume calculations were carried out for polystyrene and Lucite. Although these calculations do not always give good agreement with experiment, they represent the best quantitative

method available at this time. The procedure for calculating as a function of temperature is as follows:

(i) From specific volume data or volume expansion data, determine $v_1(T=0)$, the specific volume at absolute zero. Then from Equation (17), Chapter I, v_0, the excluded volume, is found.

(ii) Compute v^*, the reduced volume at any temperature, by dividing the specific volume at that temperature by v_0.

(iii) From the plot F versus v^* obtained by Brandt, et al. (29) for cylindrical geometry, locate the values of F corresponding to the values of v^* computed in step (ii) for several values of the scattering parameter, $P_o r_o^2$ (See Figure 14).

(iv) Using Equation (16) in Chapter I,

$$\tau_2 = \tau_0 \left[1 + F(P_o R_o^2, V^*) \right]$$

calculate τ_2 with the values of F which give the best fit to experimental data. The value of τ_0, which is the lifetime of free positrons in the material, may have to be adjusted to give a good fit.

These steps were carried out for polystyrene using the specific volume data of Alfrey, et al. (60), and for Lucite using the specific volume data of Robinson, et al. (58). Tables V and VI present the results of the theoretical calculations for polystyrene and Lucite, respectively.

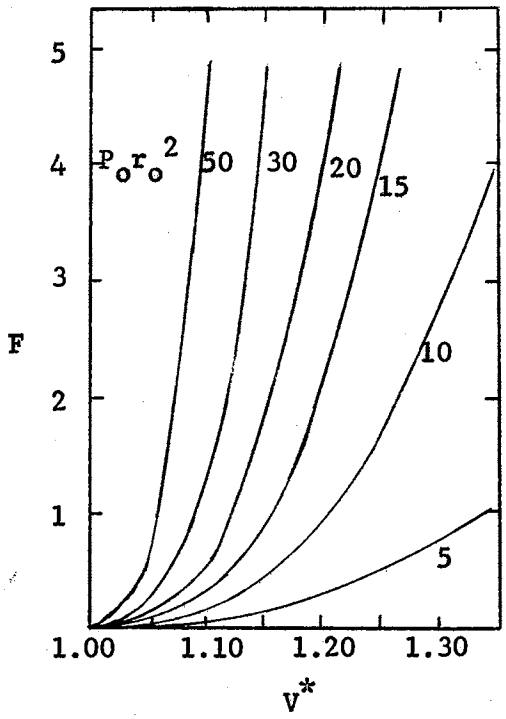

Figure 16 A Plot of the Function F Versus Reduced Volume for Cylindrical Geometry

TABLE V

THEORETICAL DATA FOR POLYSTYRENE

$\tau_o = 1.65 \times 10^{-9}$ sec. $\quad P_o r_o^2 = 5$

T (°C)	v^*	F	τ_2(ns.)
-196	1.126	0.10	1.81
- 78	1.163	0.19	1.96
0	1.186	0.25	2.06
50	1.201	0.30	2.14
80	1.213	0.35	2.23
100	1.227	0.40	2.31
120	1.241	0.45	2.39
140	1.255	0.50	2.48

TABLE VI

THEORETICAL DATA FOR LUCITE

$\tau_o = 1.5 \times 10^{-9}$ sec. $P_o r_o^2 = 5$

T (°C)	v^*	F	τ_2(ns.)
-196	1.129	0.10	1.65
- 78	1.170	0.21	1.82
0	1.200	0.30	1.95
50	1.215	0.35	2.02
80	1.227	0.40	2.10
100	1.242	0.45	2.18
120	1.255	0.50	2.25

Figures 17 and 18 show the theoretical values (solid line) and the experimental points for polystyrene and Lucite, respectively. These values have been plotted as a function of temperature rather than reduced volume, v^*, as is sometimes done. The agreement is best for Lucite. Only a few values of the parameter $P_o r_o^2$ are available for graphical computation, and the values of F for $P_o r_o^2$ between 5 and 10 might give better fits to the experimental data.

These calculations were not carried out for Marlex because the specific volume data would obviously not allow a good fit around -20°C, and because the values of F have been calculated only up to $v^* = 0.35$, which does not include the high temperature points.

Intensities

The intensity I_2 has been plotted as a function of temperature in Figures 19, 20, and 21 for polystyrene, Lucite, and Marlex, respectively.

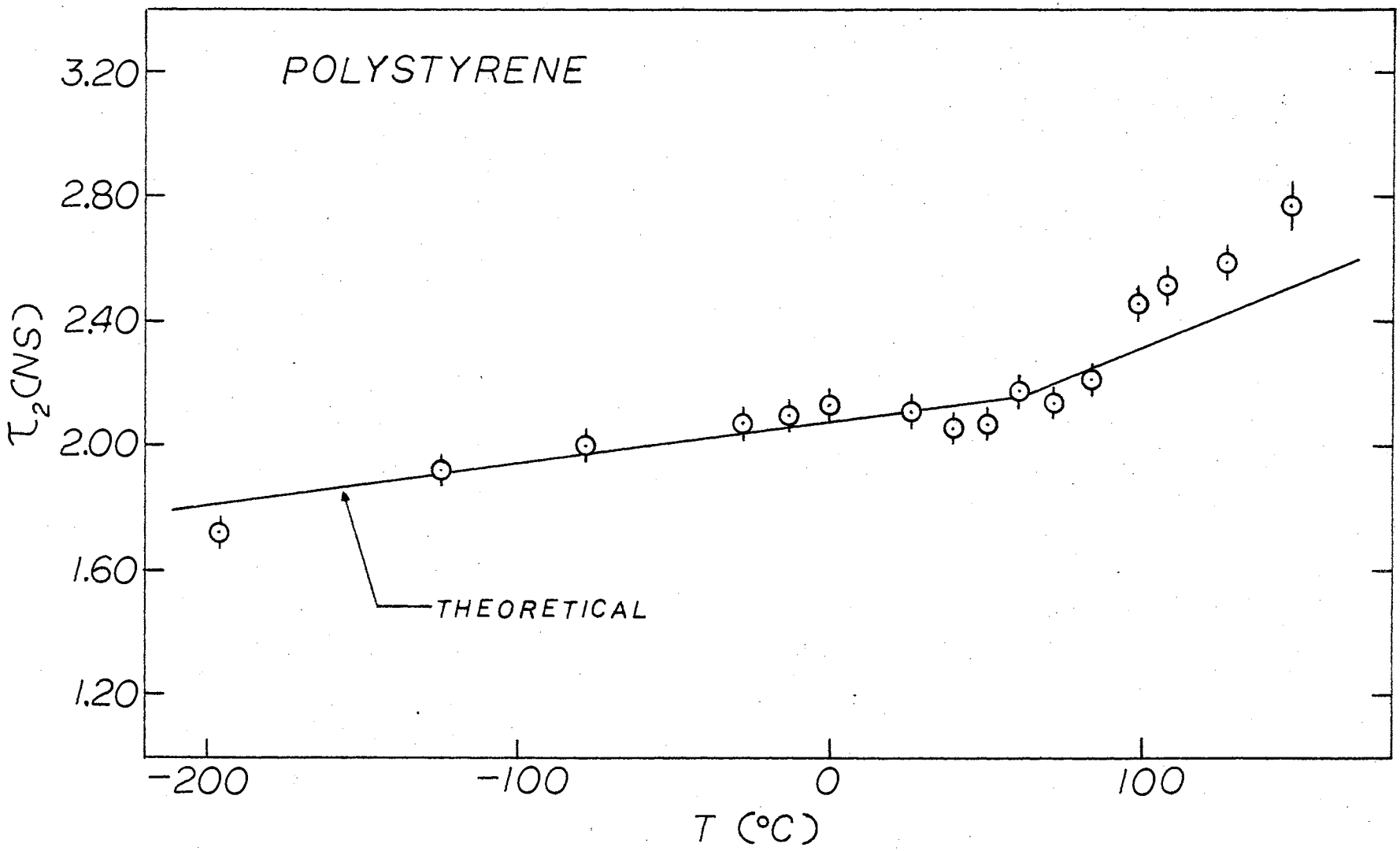

Figure 17

A Theoretical Fit to Experimental Mean Lives in Polystyrene

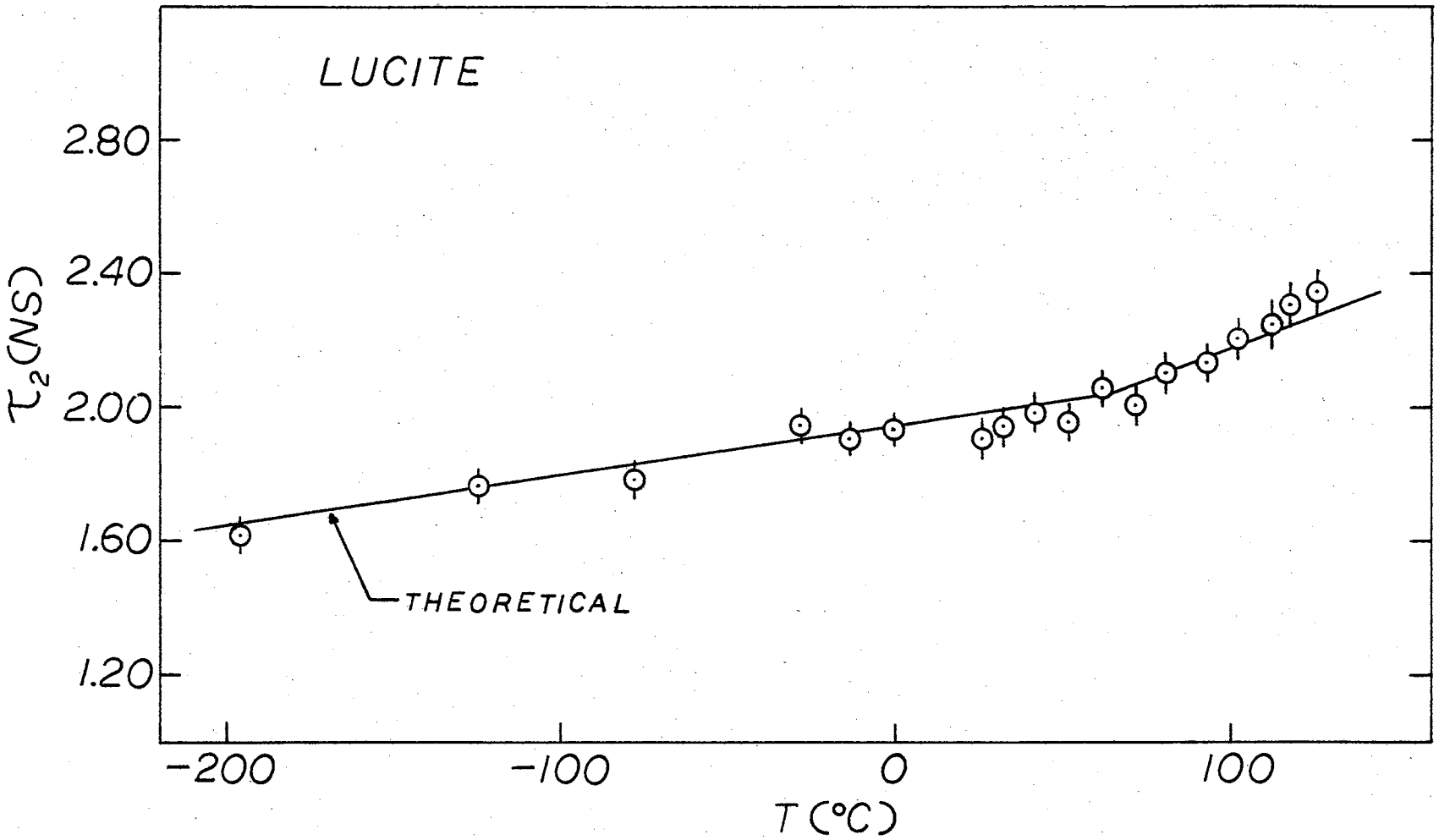

Figure 18

A Theoretical Fit to Experimental Mean Lives in Lucite

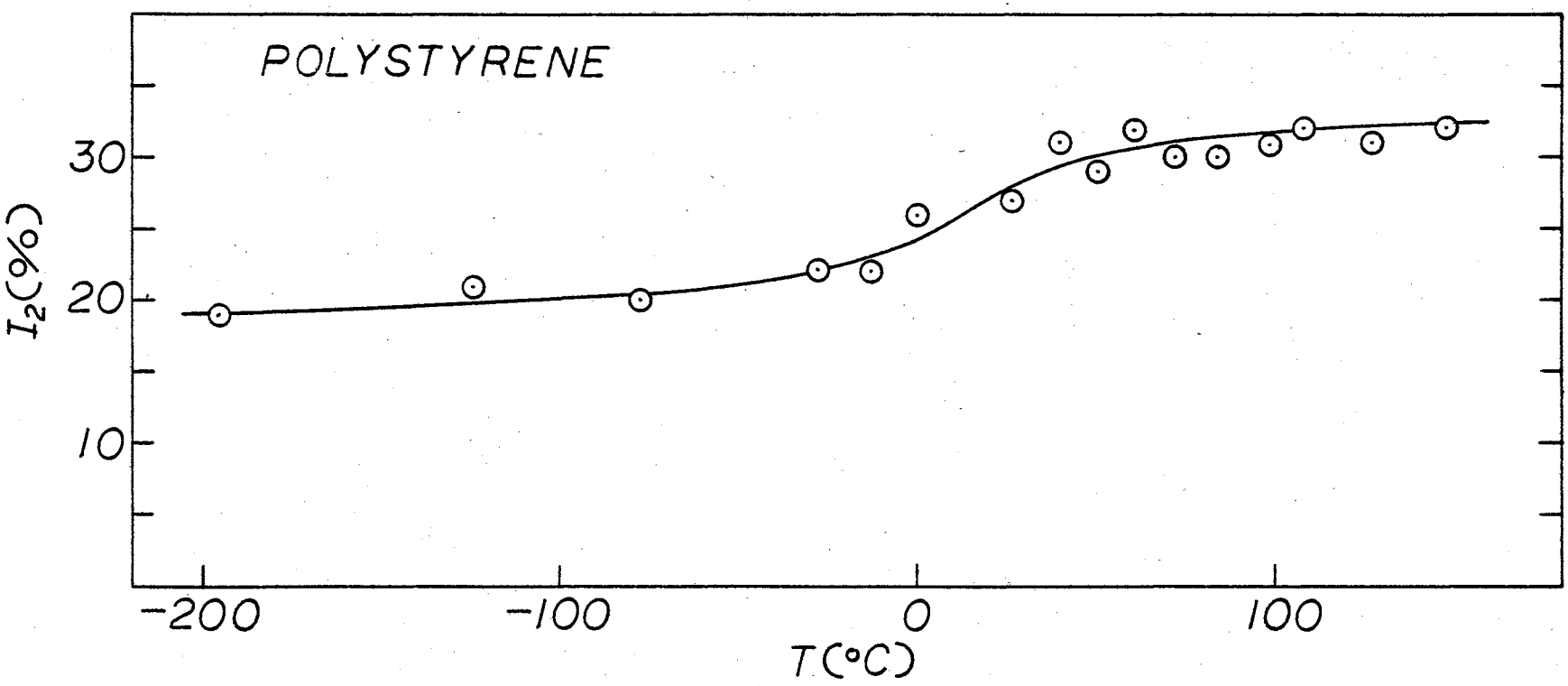

Figure 19

Intensity I_2 Versus Temperature in Polystyrene

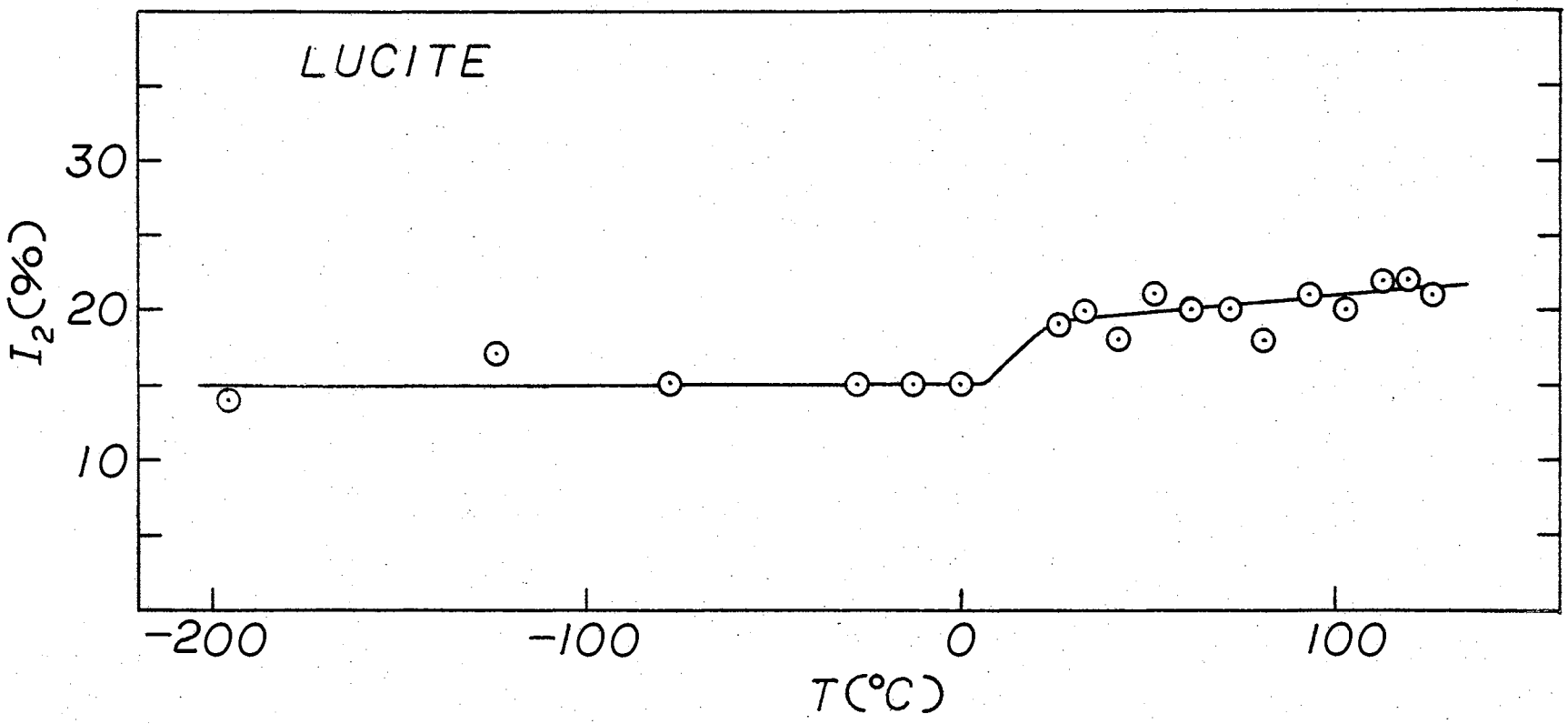

Figure 20

Intensity I_2 Versus Temperature in Lucite

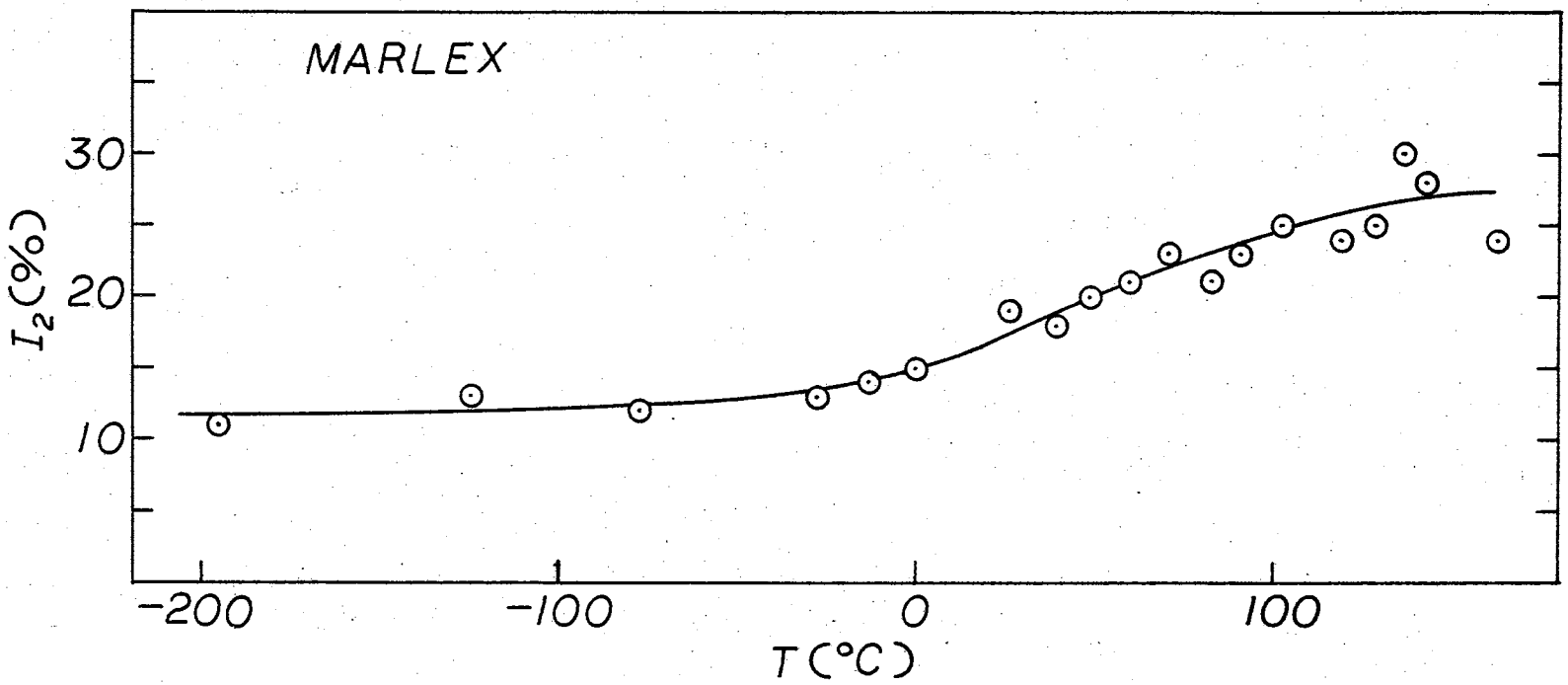

Figure 21

Intensity I_2 Versus Temperature in Marlex 50

Due to the small changes in I_2, it would be difficult to draw any conclusions about the shape of the I_2 variation, but there is a general increase in intensity with temperature for all three materials, which has been indicated on the figures with a solid line which visually fits the points. The error in all cases is plus or minus five per cent.

Positrons in polystyrene show an increase in I_2 of 13%, from 19% at -196°C to 32% at +148°C. The maximum increase of I_2 in Lucite is 8%, and the maximum increase in Marlex is 19%, from 11% at -196°C to 30% at +136°C. There is no sharp change in I_2 in Marlex at -20°C corresponding to the change in τ_2.

As was mentioned in Chapter I, singlet positronium is formed in a fraction 1/3 I_2, so the maximum changes in amount of positronium formed is about 17% in polystyrene, 11% in Lucite, and 25% in Marlex. The free volume of high density polyethylene increases by about 25% from -200°C to melting (of which only about 8% is attributable to the crystalline regions), and the free volume of Lucite increases by about 10% from -200°C to +120°C, both of these figures being comparable to the increases in amounts of positronium formed in them. Polystyrene, however, undergoes only a 10% or 11% change in free volume from -200°C to +150°C. Increasing or decreasing the temperature enlarges the "holes" or squeezes them shut, respectively, thereby changing the probability of positronium formation as well as the value of τ_2. Another way of explaining the increase of I_2 with temperature involves changes in the width of the Ore gap, which was discussed in Chapter I.

High and Low Density Samples

The data of Table IV fulfills its purpose; it shows two samples of the same plastic may have widely different values of τ_2. The τ_2 variation of these samples at other temperatures would undoubtedly also differ.

Another interesting point is that there might be a simple correlation between room temperature mean life and density, but for these samples the ratio of lifetimes is about 1.13, and the ratio of densities only 1.04. A rough free volume calculation gives about 18% for the low density sample and 16% for the high density sample and a ratio of 1.12. This shows that the lifetime difference is more consistent with the free volume difference.

Graphite

The structure of the graphite crystal is unfavorable to the formation of positronium. It consists (61) of hexagonal layers of molecules separated by 3.40 Å. This distance is large enough that there can be no covalent bonds between layers. The superimposed giant layer molecules are held together only by weak van der Waals forces.

The lowest discrete energy of the positronium atom will become positive if its wave function is confined within a sphere of radius $\sim \leq 1.8\ a_p$, where a_p is the positronium radius, about an angstrom (25). Even excluding the small radii of the carbon atoms, a sphere of radius 1.8 Å could not be fit in the interplanar spaces of graphite. It is actually only necessary to decrease the binding energy of positronium until there is no Ore gap left in order that all annihilations

take place in the free state.

Conclusion

It is hoped that more τ_2 and I_2 data on high density polyethylene over a similar temperature range will be forthcoming in the near future. It would doubtless be helpful to have on hand the results of other physical measurements on the polymer for comparison, such as infra - red spectra, x-ray diffraction patterns, and dilatometric specific volume data. Perhaps no one of these alone would be sufficient.

In order to draw more meaningful conclusions about the relationship of τ_2 and I_2 to free volume changes and lattice transitions, it is suggested that materials whose properties are known to undergo large and abrupt changes be used for positron annihilation samples. An example is hexatriacontane, $C_{36}H_{74}$, which undergoes a sudden lattice contraction at about -50°C, and a specific volume increase of at least 10 per cent in less than a 10 degree interval at +70°C (45).

Another worthwhile study would be an attempt to increase the amounts of positronium formed in materials through heat treatment or exposure to radiation, or to induce by these methods positronium to form in materials in which it is ordinarily not formed.

BIBLIOGRAPHY

1. Dirac, P.A.M. Proceedings Cambridge Philosophical Society 26, 361 (1930).

2. Wheeler, J.A. Annals of the New York Academy of Sciences 48, 219-238 (1946).

3. Mohorovicic, S. Astron. Nacht 253, 94 (1934).

4. Ruark, A.E. Physical Review 68, 278 (1945).

5. Ore, A. and J.L. Powell. Physical Review 75, 1696-1699 (1949).

6. Simons, Lennart. Encyclopedia of Physics 34, 139-165 (1958). Springer, Berlin.

7. De Benedetti, S. and H.C. Corben. Annual Review of Nuclear Science 4, 191-218 (1954).

8. Michel, L. Nuovo Cimento 10, 319-324 (1953).

9. Deutsch, M. Progress in Nuclear Physics 3, 131-158 (1953).

10. Shearer, J.W. and M. Deutsch. Physical Review 76, 462 (1949).

11. Deutsch, M. Physical Review 82, 455-456 (1951).

12. Deutsch, M. Physical Review 83, 866 (1951).

13. Bell, R.E. and R.L. Graham. Physical Review 90, 644-654 (1953).

14. Siegbahn, K. Beta - and Gamma - Ray Spectroscopy. New York: Interscience Publishers, Inc. (1955).

15. Wallace, P.R. Solid State Physics 10, 1-69 (1960).

16. Graham, R.L. and A.T. Stewart. Canadian Journal of Physics 32, 678-679 (1954).

17. Dresden, M. Physical Review 93, 1413-1414 (1954).

18. Garwin, R.L. Physical Review 91, 1571-1572 (1953).

19. Ferrell, R.A. Reviews of Modern Physics 28, 308-337 (1956).

20. Wallace, P.R. Physical Review 100, 738-741 (1955).

21. Green, R.E. and R.E. Bell. Canadian Journal of Physics 35, 398-409 (1957).

22. Bell, R.E. and M.H. Jørgensen. Canadian Journal of Physics 38, 652-664 (1960).

23. Bisi, A., et al. Physical Review Letters 5, 59-60 (1960).

24. Lee-Whiting, G.E. Physical Review 97, 1557-1558 (1955).

25. De Benedetti, S., et al. Physical Review 77, 205-212 (1950).

26. Landes, H.S., S. Berko, and A.J. Zuchelli. Physical Review 103, 828-829 (1957).

27. Stump, R. Bulletin of the American Physical Society Series II, 2, 173 (1957).

28. De Zafra, R.L. and W.T. Joyner. Physical Review 112, 19-29 (1958).

29. Brandt, W., S. Berko, and W.W. Walker. Physical Review 120, 1289-1295 (1960).

30. Simms, P.C. Review of Scientific Instruments 32, 894 (1961).

31. Deutsch, M. Methods of Experimental Physics, Vol. 5B. Ed. L. Marton. New York: Academic Press, Inc. (1955).

32. Bell, R.E., R.L. Graham, and H.E. Petch. Canadian Journal of Physics 30, 35-49 (1951).

33. Katz, L. and A.S. Penfold. Reviews of Modern Physics 24, 28-44 (1952).

34. Billmeyer, F.W. Jr. Textbook of Polymer Chemistry. New York: Interscience Publishers, Inc. (1957).

35. Tobolsky, A.V. Properties and Structure of Polymers. New York: John Wiley, Inc. (1960).

36. Fleck, H.R. Plastics - Scientific and Technological. New York: Chemical Publishing Co., Inc. (1949).

37. Fox, T.G. and P.J. Flory. Journal of Applied Physics 21, 581-591 (1950).

38. Jones, R.V. and P.J. Boeke. Industrial and Engineering Chemistry 48, 1155-1161 (1956).

39. Smith, D.C. Industrial and Engineering Chemistry 48, 1161-1164 (1956).

40. Raff, R.A.V. and J.B. Allison. Polyethylene. New York: Interscience Publishers, Inc. (1956).

41. Swan, P.R. Journal of Polymer Science 56, 403-407 (1962).

42. Holmes, D.R. Journal of Polymer Science 42, 273-274 (1960).

43. Swan, P.R. Journal of Polymer Science 42, 525-534 (1960).

44. Matsuoka, S. Journal of Polymer Science 57, 580 (1962).

45. Cole, E.A. and D.R. Holmes. Journal of Polymer Science 46, 245-256 (1960).

46. Danusso, F., G. Moraglia, and G. Talamini. Journal of Polymer Science 21, 139-140 (1956).

47. Ohlberg, S.M. and S.S. Fenstermaker. Journal of Polymer Science 32, 514-516 (1958).

48. Kohonen, T. Ann. Acad. Scient. Fenn 92, 1-76 (1961).

49. Fabri, G., E. Germagnoli, and G. Randone. Physical Review 130, 204-205 (1963).

50. Newton, T.D. Physical Review 78, 490 (1950).

51. Bacon, R.H. American Journal of Physics 21, 428 (1953).

52. Beers, Y. Introduction to the Theory of Error. Cambridge, Mass.: Addison-Wesley Publishing Co., Inc. (1953).

53. Bay, Z., V.P. Henri, and H. Kanner. Physical Review 100, 1197-1208 (1955).

54. Loper, G.D. The Variation of the Anomalous Positron Lifetime With Temperature in Solids. Unpublished M.S. Thesis, Oklahoma State University, 1962.

55. Pigg, J.L. Private Communication, 1963.

56. Wilson, R.K., P.O. Johnson, and R. Stump. Physical Review 129, 2091-2095 (1963).

57. Bondi, A. Journal of Physical Chemistry 58, 929-939 (1954).

58. Robinson, H.A., R. Ruggy, and E. Slanty. Journal of Applied Physics 15, 343-351 (1944).

59. Boyer, R.F., and R.S. Spencer. Journal of Applied Physics 16, 594-607 (1945).

60. Alfrey, T., G. Goldfinger, and H. Mark. Journal of Applied Physics 14, 700 (1943).

61. Pauling, L. The Nature of the Chemical Bond. Ithaca, New York: Cornell University Press (1960).

APPENDIX A

Basic Equations for Delayed Coincidence Experiments

If f(t) is the time distribution to be measured and P(x) the prompt resolution curve, the distribution given by the measurement is

$$F(x) = \int_{-\infty}^{+\infty} f(t)\, P(x-t)\, dt.$$

In the simplest case, when only a single decay is involved with mean life $\tau = \frac{1}{\lambda}$,

$$f(t) = \lambda e^{-\lambda t} \qquad t > 0$$

$$f(t) = 0 \qquad t \leq 0$$

$$F(X) = \lambda \int_0^{\infty} e^{-\lambda t}\, P(x-t)\, dt.$$

Differentiation with respect to x gives

$$\frac{dF(x)}{dx} = \lambda \left[P(x) - F(x) \right]$$

$$\frac{d \ln F(x)}{dx} = -\lambda \left[1 - \frac{P(x)}{F(x)} \right] \cong -\lambda$$

when $F(x) >> P(x)$. In the polymers, P(x) is not much altered in form by the shorter component of f(t). There is a region in which $F(x) >> P(x)$ for the longer component, and in this region τ_2 is obtained from the logarithmic slope of the tail of the time distribution (48).

APPENDIX B

The Weighted Least Squares Fit

This is a problem of fitting a straight line to n points $(x_1\ y_1)$, $(x_2\ y_2)$, --- $(x_n\ y_n)$ for which the standard deviation of y, σ_Y , varies from point to point and x is known exactly.

The data were plotted in semilog coordinates, so that

$$Y_i = \ln_e N_i$$

where N_i is the number of coincidence counts of the i^{th} point. Also, x_i represents the i^{th} channel, or i^{th} time point.

Let

$$N_1 \sigma_{Y_1}^2 = N_2 \sigma_{Y_2}^2 = \cdots = N_m \sigma_{Y_m}^2 = \sigma^2$$

where the N's, called weights, are the ratios of the variances at each point to some convenient variance, σ^2 , taken as a standard of reference.

A line among the n points such that the sum of the squares of the vertical distances between each point and the line is a minimum is wanted; i.e., an equation of the form

$$Y = \lambda X + b$$

where λ is the slope and b the y intercept. Denote the vertical height between each point and the line by h_1, h_2, --- h_n. Now and b are to be chosen such that

$$\sum_{i=1}^{n} \left(\frac{h_i}{\sigma_Y}\right)^2 = \frac{1}{\sigma^2} \sum_{i=1}^{n} N_i h_i^2 = \text{minimum.}$$

This means

$$\frac{\partial}{\partial \lambda} \sum_{i=1}^{n} N_i h_i^2 = 2 \sum_{i=1}^{n} N_i h_i \frac{\partial h_i}{\partial \lambda} = 0 \; ; \; \sum_{i=1}^{n} N_i h_i \frac{\partial h_i}{\partial \lambda} = 0$$

$$\frac{\partial}{\partial b} \sum_{i=1}^{n} N_i h_i^2 = 2 \sum_{i=1}^{n} N_i h_i \frac{\partial h_i}{\partial b} = 0 \; ; \; \sum_{i=1}^{n} N_i h_i \frac{\partial h_i}{\partial b} = 0 .$$

With the equation

$$\sum_{i=1}^{n} N_i h_i = \sum_{i=1}^{n} N_i Y_i - b \sum_{i=1}^{n} N_i - \lambda \sum_{i=1}^{n} N_i X_i$$

it is seen that

$$\frac{\partial h_i}{\partial b} = -1 \quad , \quad \frac{\partial h_i}{\partial \lambda} = - X_i .$$

The two normal equations become

$$- \sum_{i=1}^{n} N_i h_i \frac{\partial h_i}{\partial b} = \sum_{i=1}^{n} N_i h_i = \sum_{i=1}^{n} N_i Y_i - b \sum_{i=1}^{n} N_i - \lambda \sum_{i=1}^{n} N_i X_i = 0$$

$$- \sum_{i=1}^{n} N_i h_i \frac{\partial h_i}{\partial \lambda} = \sum_{i=1}^{n} N_i X_i h_i = \sum_{i=1}^{n} N_i X_i Y_i - b \sum_{i=1}^{n} N_i X_i - \lambda \sum_{i=1}^{n} N_i X_i^2 = 0.$$

These are two simultaneous equations in two unknowns, λ and b.

The solutions are

$$\lambda = \frac{\sum N_i \sum N_i X_i Y_i - \sum N_i X_i \sum N_i Y_i}{\sum N_i \sum N_i X_i^2 - \left(\sum N_i X_i \right)^2} = \frac{\sum N_i (X_i - \bar{X})(Y_i - \bar{Y})}{\sum N_i (X_i - \bar{X})^2}$$

and

$$b = \frac{\sum N_i Y_i \sum N_i X_i^2 - \sum N_i X_i \sum N_i X_i Y_i}{\sum N_i \sum N_i X_i^2 - \left(\sum N_i X_i \right)^2} = \frac{\bar{Y} \sum N_i X_i^2 - \bar{X} \sum N_i X_i Y_i}{\sum N_i (X_i - \bar{X})^2}$$

where

$$\bar{X} = \sum_{i=1}^{\tilde{n}} N_i X_i \Big/ \sum_{i=1}^{\tilde{n}} N_i \quad , \qquad \bar{Y} = \sum_{i=1}^{\tilde{n}} N_i Y_i \Big/ \sum_{i=1}^{\tilde{n}} N_i \quad .$$

APPENDIX C

Fortran Program for Calculation of τ_2

In the program, the terms in the statements are to be interpreted as follows:

COUNT (I) ----- N_i, number of coincidence counts

CHANN (I) ----- x_i, the channel number

LOGEF (COUNT (I)) ----- y_i, natural log of N_i

AVERC ----- $\bar{x}$

AVERY ----- $\bar{y}$

SLOPE ----- λ

TAU2 ----- τ_2, the mean life

YINT ----- b

STDEV ----- σ , the square root of the variance

CALCN ----- k, the calibration constant

IDENT ----- the identity number, or data run number.

All the symbols are the ordinary Fortran symbols.

```
 1  DIMENSION     COUNT (50),  CHANN (50)
 2  SUM 1 = 0.0
 3  SUM 2 = 0.0
 4  SUM 3 = 0.0
 5  SUM 4 = 0.0
 6  SUM 5 = 0.0
 7  SUM 6 = 0.0
 8  READ 1, N, IDENT, CALCN
 9  DO 13    I = 1,N
10  READ 2, COUNT (I), CHANN (I)
11  SUM 1 = SUM 1 + COUNT (I)
12  SUM 2 = SUM 2 + COUNT (I) * CHANN (I)
13  SUM 3 = SUM 3 + COUNT (I) * LOGEF (COUNT (I))
14  AVERC = SUM 2/SUM 1
15  AVERY = SUM 3/SUM 1
16  DO  19   I = 1,N
17  SUM  4 = SUM 4 + COUNT (I) * (CHANN (I) - AVERC) * (LOGEF (COUNT
    (I)) - AVERY)
18  SUM  5 = SUM 5 + COUNT (I) * ((CHANN (I) - AVERC) ** 2)
19  SUM  6 = SUM 6 + AVERY * COUNT (I) * (CHANN (I) ** 2) - AVERC *
    COUNT (I) * CHANN (I) * LOGEF (COUNT (I))
20  SLOPE = SUM 4/SUM 5
21  TAU2 = (-1.00 / SLOPE) * CALCN
22  YINT = SUM 6/SUM 5
23  STDEV = SQRTF (((1.00 / SLOPE) ** 4)/SUM 5) * CALCN
24  PUNCH 1, SLOPE, TAU2, YINT, STDEV, IDENT
25  PAUSE 1
26  GO TO 2
    END
```

VITA

Gerald Dean Loper, Jr.

Candidate for the Degree of

Doctor of Philosophy

Thesis: THE EFFECT OF TEMPERATURE ON THE FORMATION AND ANNIHILATION OF POSITRONIUM IN POLYMERS

Major Field: Physics

Biographical:

Personal Data: Born May 4, 1937, in Brooklyn, New York, the son of Johanna L. and Gerald D. Loper.

Education: Attended grade school in Brooklyn and Wichita, Kansas; graduated from Wichita High School East in 1955; conducted undergraduate studies at the University of Arizona and the University of Wichita; received the Bachelor of Arts degree from the latter institution with a major in Physics in May 1959; started graduate studies in Physics at Oklahoma State University on a National Defense Education Act Fellowship in 1959; received the Master of Science degree there with a major in Physics in May 1962; completed requirements for the Doctor of Philosophy degree in August 1964.

Professional experience: Was Instructor of Physics at Southwestern College in Winfield, Kansas, summer 1959, and is currently Assistant Professor of Physics at Wichita State University.